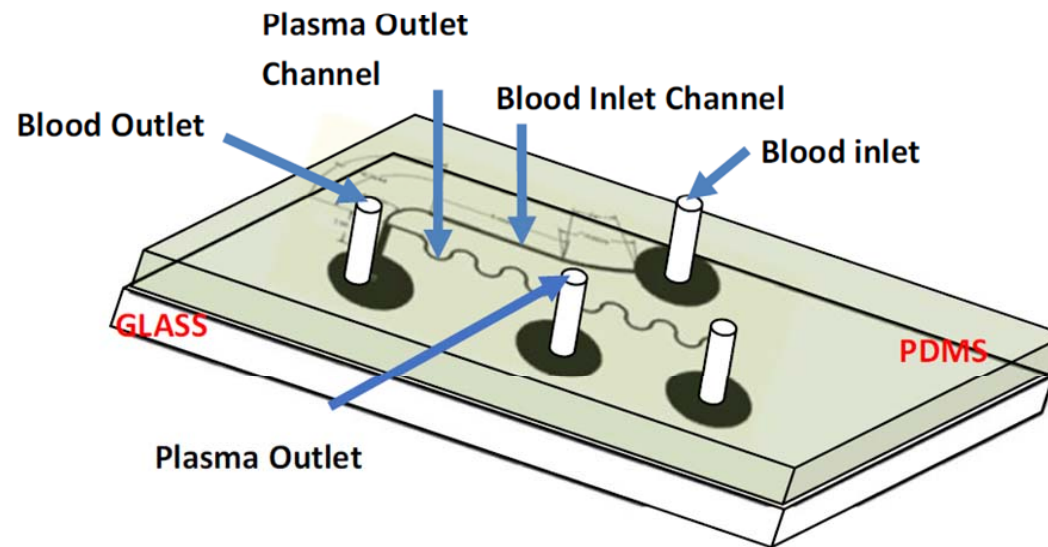


Development of Innovative Bio-Microdevices



Amit Agrawal

Microfluidics Lab, Department of Mechanical Engineering, Indian Institute of Technology Bombay

Prof. H.H. Mathur Award for Excellence in Applied Sciences

IIT Bombay, 27 February 2018

Outline of the talk

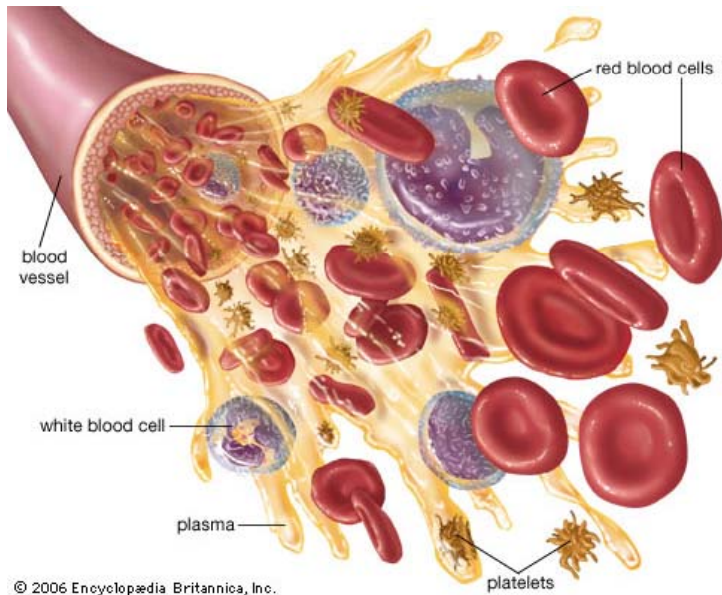
- Development of Innovative Bio-microdevices
 - Blood plasma separation microdevice
 - Three-dimensional hydrodynamic focusing device
- Looking beyond the Navier-Stokes equations
 - First analytical solution of Burnett equations
 - Derivation of Onsager-Burnett equations
- Conclusions

Development of Blood-Plasma-Separation Microdevice

Why separate plasma from blood?

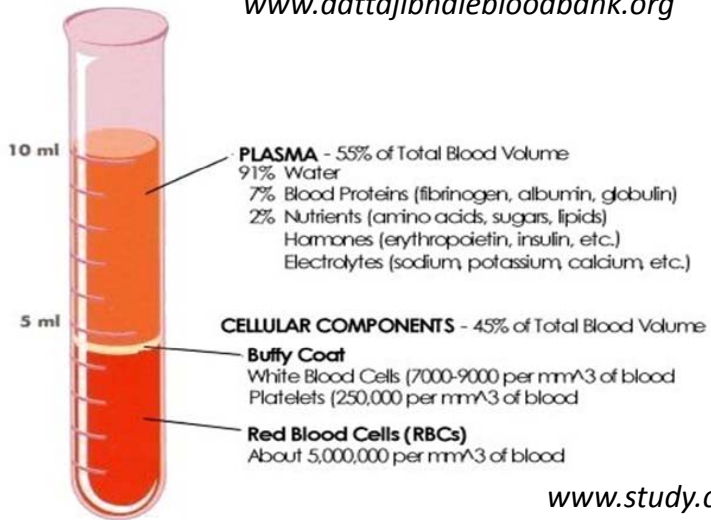
- Many blood tests are carried out on plasma
- Plasma has plenty of **biomarkers** and **analytes** – indicators of human body functioning
- **Efficient detection of these analytes requires separation of cells** – as cells may interfere with analysis
- Separation of plasma from blood is an **indispensable process** for disease diagnostics

Constituents of Human Blood



© 2006 Encyclopædia Britannica, Inc.

www.dattajibhalebloodbank.org



www.study.com

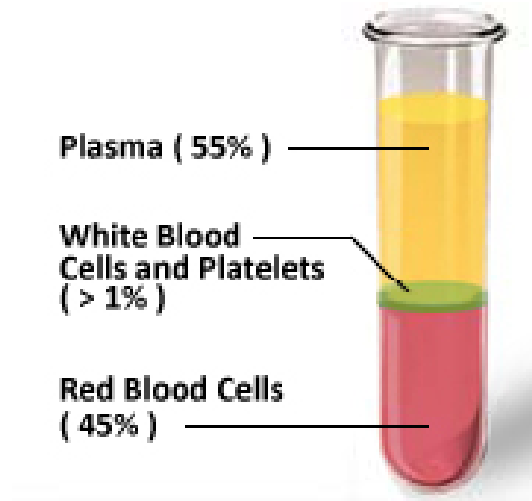
Constituents	% of whole blood	Typical size (µm)	Normal count (per µL)
RBC	45-50	7-9	4.5 – 5.5 million
WBC	1	8-18	5000 - 8000
Platelets		2.5	250,000 - 300,000
Plasma	Rest	NA	NA

Conventional Method for Separating Plasma from Blood



Centrifuge

www.pocdsscientific.com.au



www.pennmedicine.org

➤ Centrifugation

Issues: Labor intensive, time consuming, multiple stages of blood handling, prone to errors

Microfluidics offers a platform to bring all stages of processing (plasma separation, tests, etc) into a single micro-device!

Lab-on-a-Chip device



Blood-plasma separation microdevice @ IIT Bombay

Advantages of point-of-care micro-device

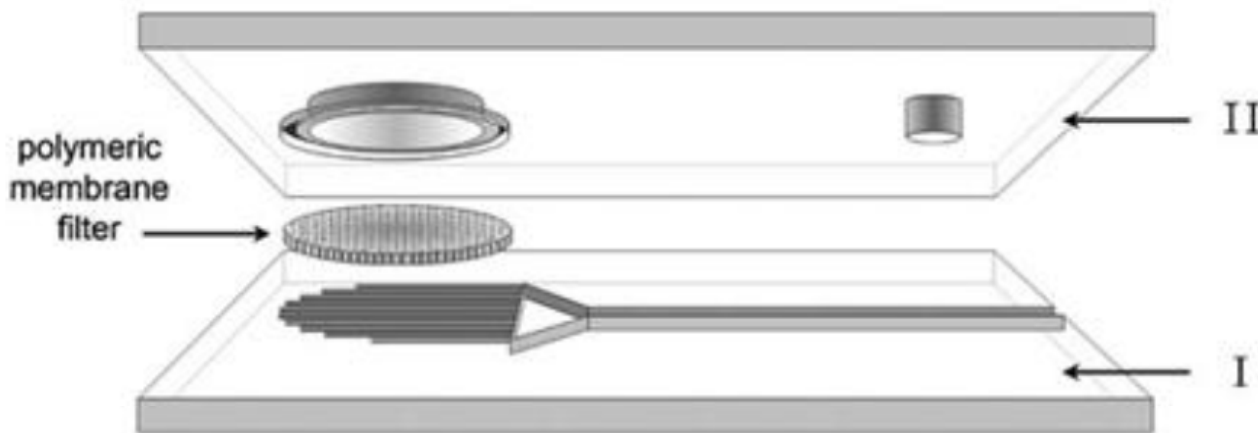
- **Reduces size** of functionally critical components of analytical systems
- **Small sample amount/** less consumption of costly reagents
- **Quick and accurate analysis** – reduces multiple stages of manual handling, minimal errors
- **Portability** – Can be used even in very remote areas – carry in your pocket!
- **Bed site testing** – reduction in transportation time

Filtration based devices in Literature

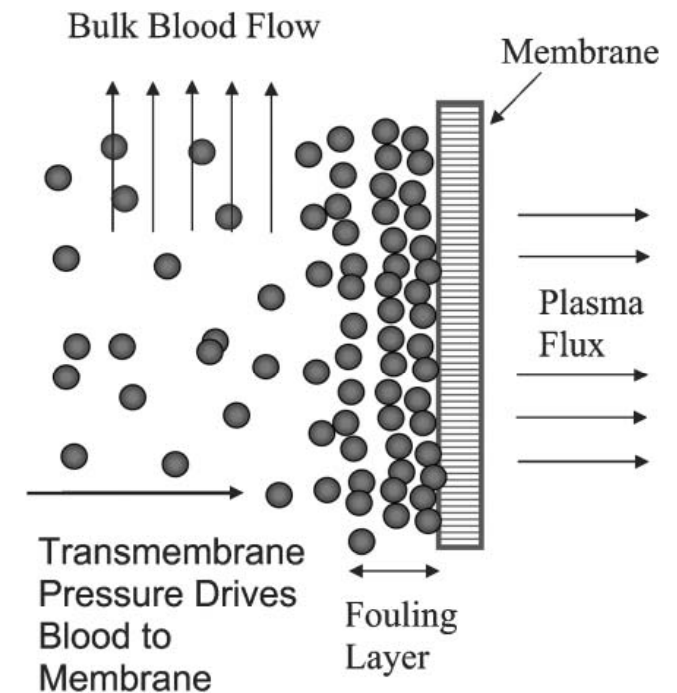
If particles are rigid – will not be able to pass through pores smaller than their size

Depending upon the point of plasma extraction

- Dead End Filtration
- Cross Flow Filtration

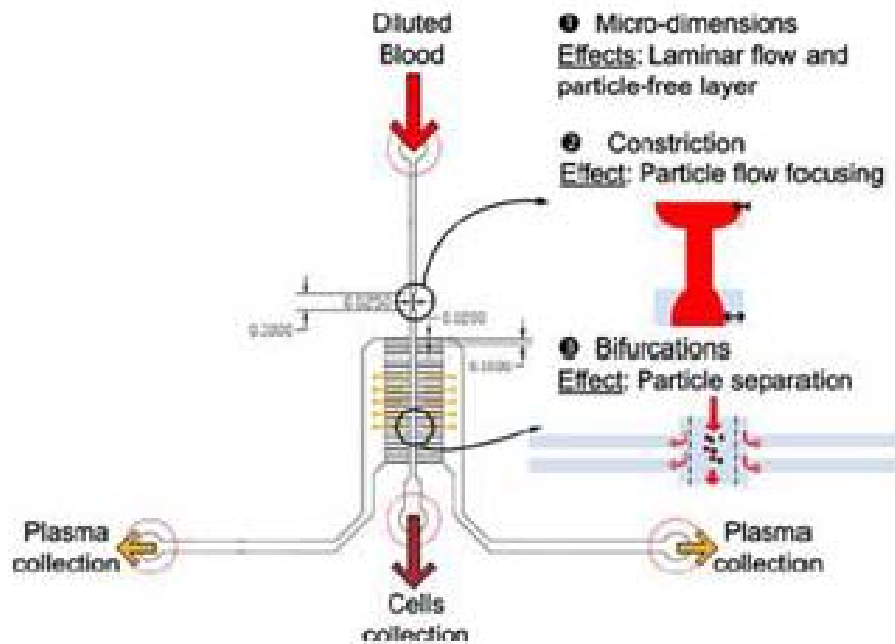


Thorslund, S., Klett, O., Nikolajeff, F., Markides, K., & Bergquist, J. (2006). A hybrid poly (dimethylsiloxane) microsystem for on-chip whole blood filtration optimized for steroid screening. *Biomedical Microdevices*, 8(1), 73-79.

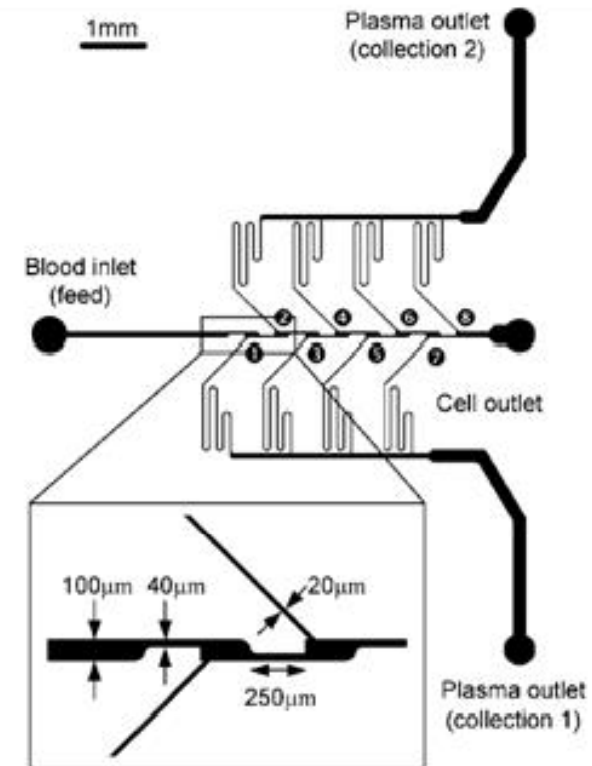


Crowley, T. A., & Pizziconi, V. (2005). Isolation of plasma from whole blood using planar microfilters for lab-on-a-chip applications. *Lab on a Chip*, 5(9), 922-929.

Hybrid Designs (from Literature)



Kersaudy-Kerhoas, M., Dhariwal, R., Desmulliez, M. P., & Jovet, L. (2010). Hydrodynamic blood plasma separation in microfluidic channels. *Microfluidics and Nanofluidics*, 8(1), 105-114.



Kersaudy-Kerhoas, M., Kavanagh, D. M., Dhariwal, R. S., Campbell, C. J., & Desmulliez, M. P. (2010). Validation of a blood plasma separation system by biomarker detection. *Lab on a Chip*, 10(12), 1587-1595.

Issues with the existing designs

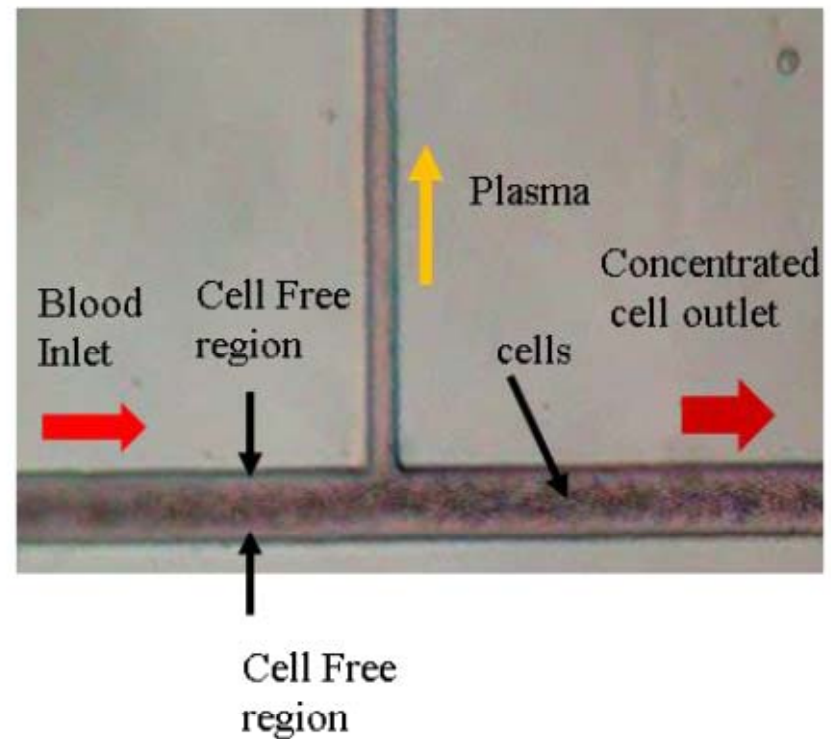
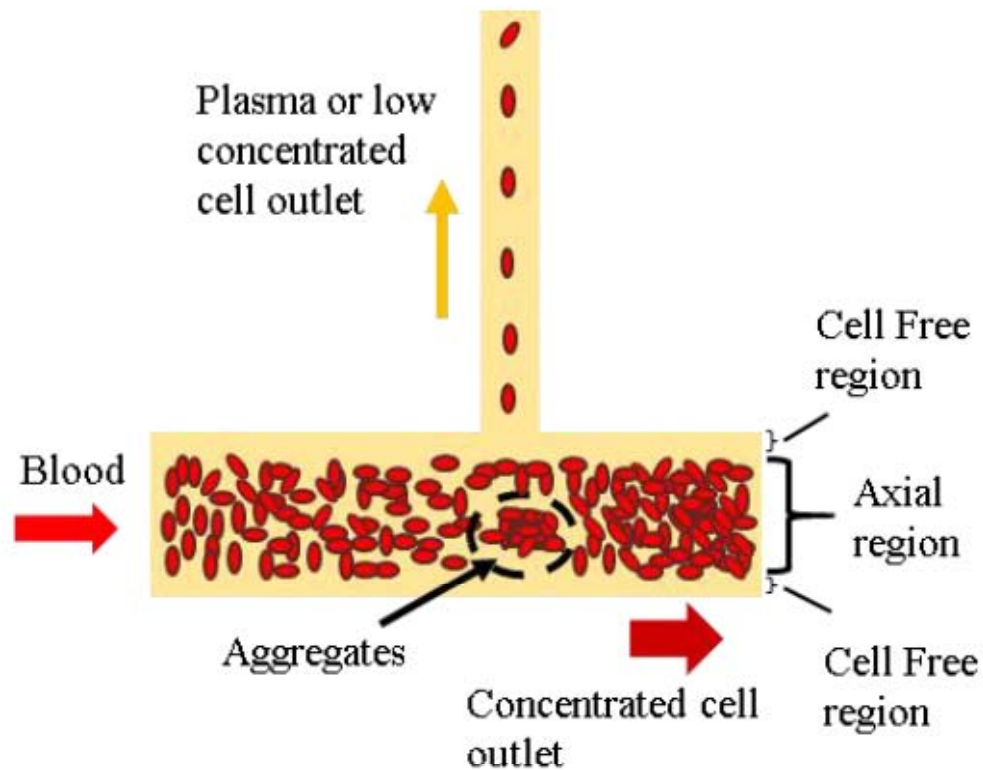
- Most designs demonstrated on diluted blood
- Small feature sizes
 - Dimensional tolerances become critical
 - Difficult to manufacture
 - Prone to clogging
- Low rate of plasma extraction

Can the design be simplified?

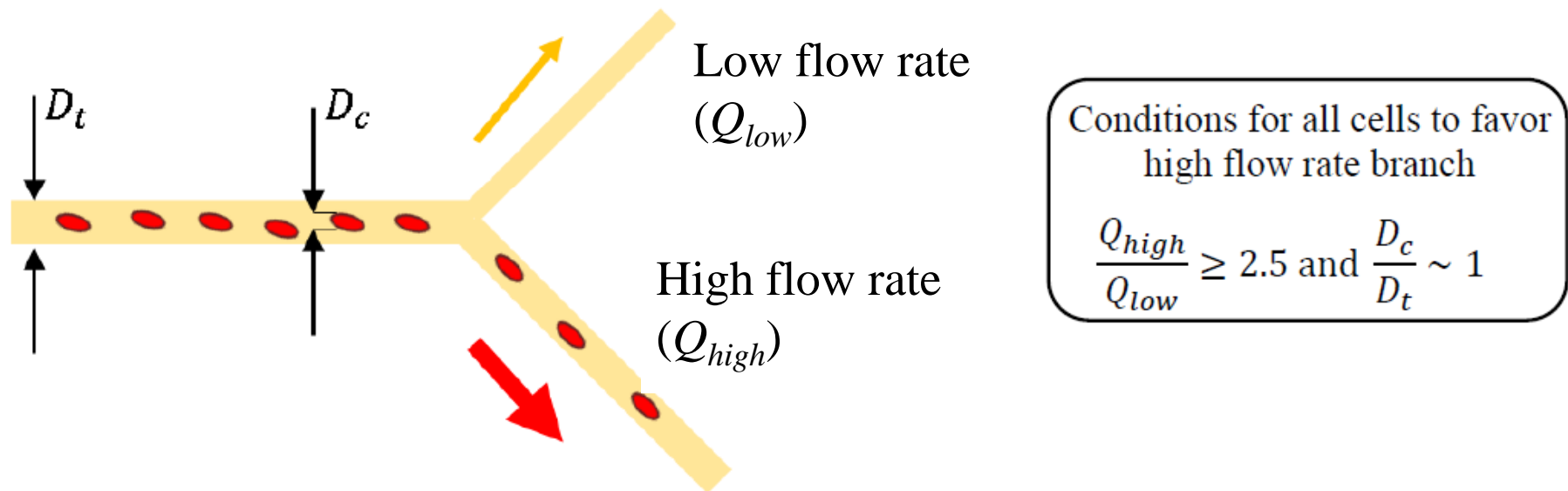
Tripathi et al., *J Micromechanics and Microengineering*,
Vol. 25, 083001, 2015. (Invited review)

Bio-Physical effects: Fahraeus effect

Fahraeus effect in a simple T shaped microchannel

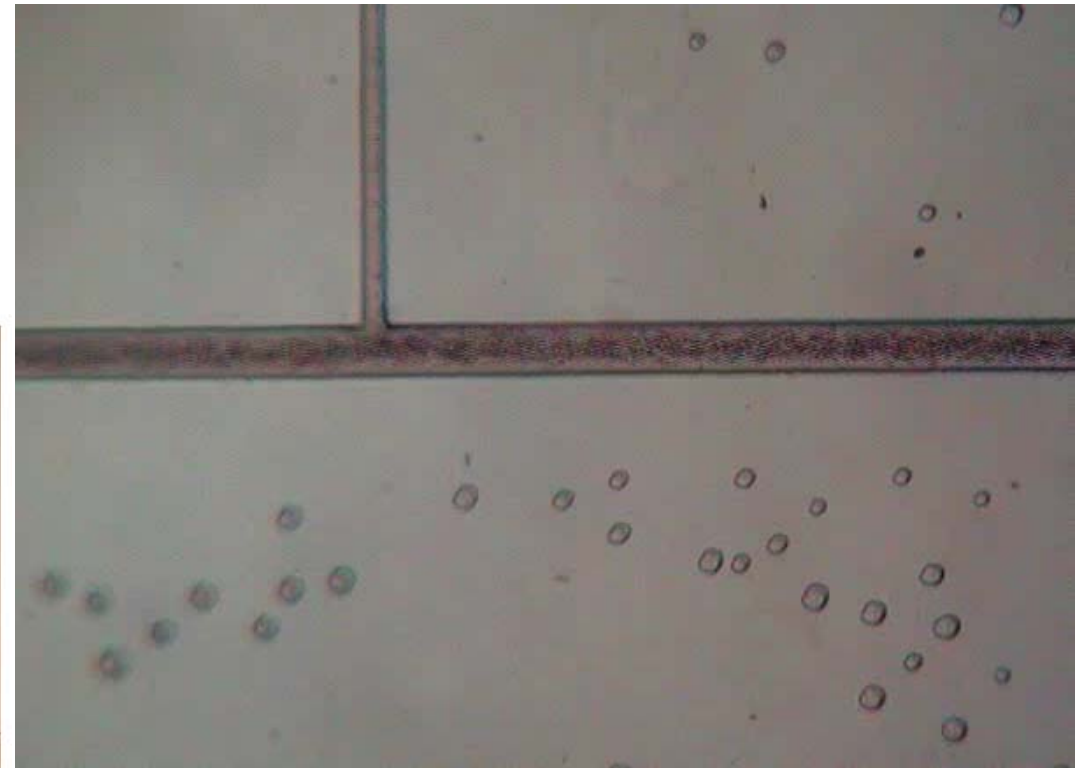
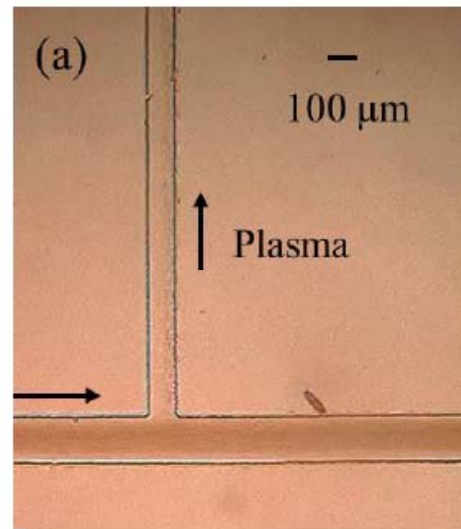
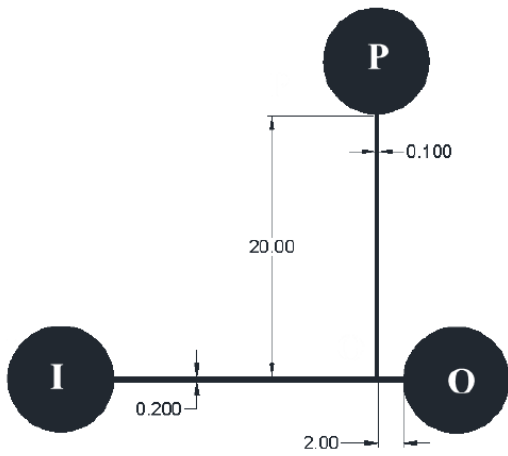


Bio-Physical effect: Zweifach – Fung Bifurcation Law

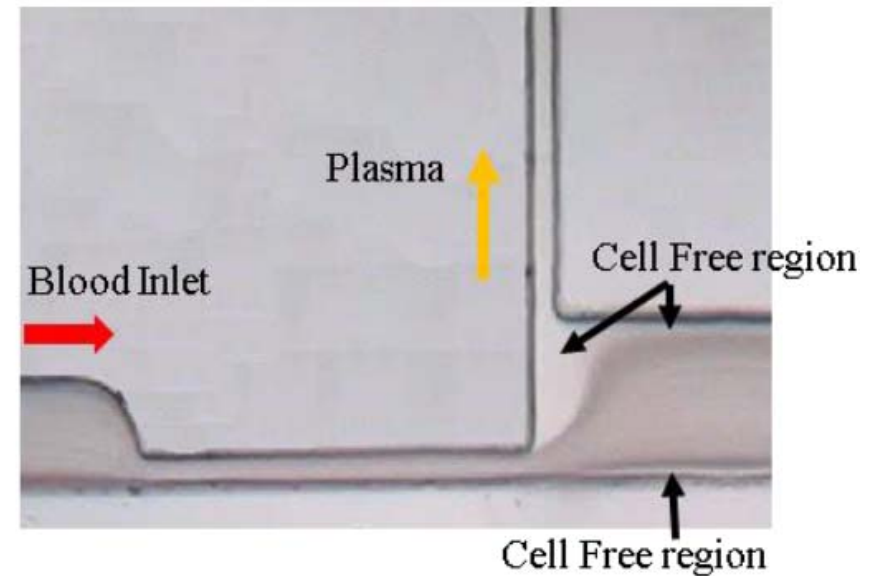
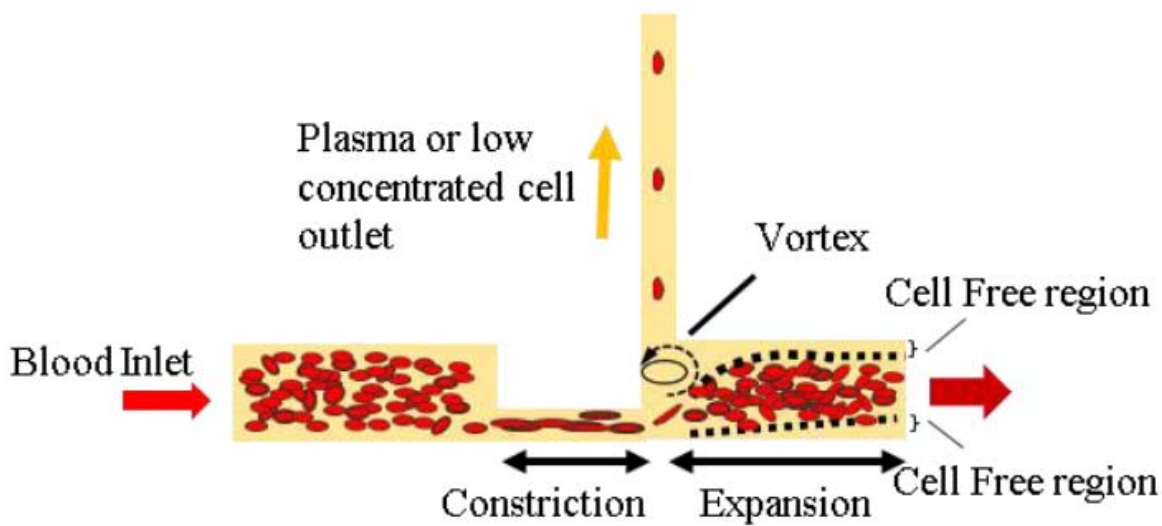


- **Corner stone** of most hydrodynamic based microfluidic devices

Separation using a simple T-microchannel

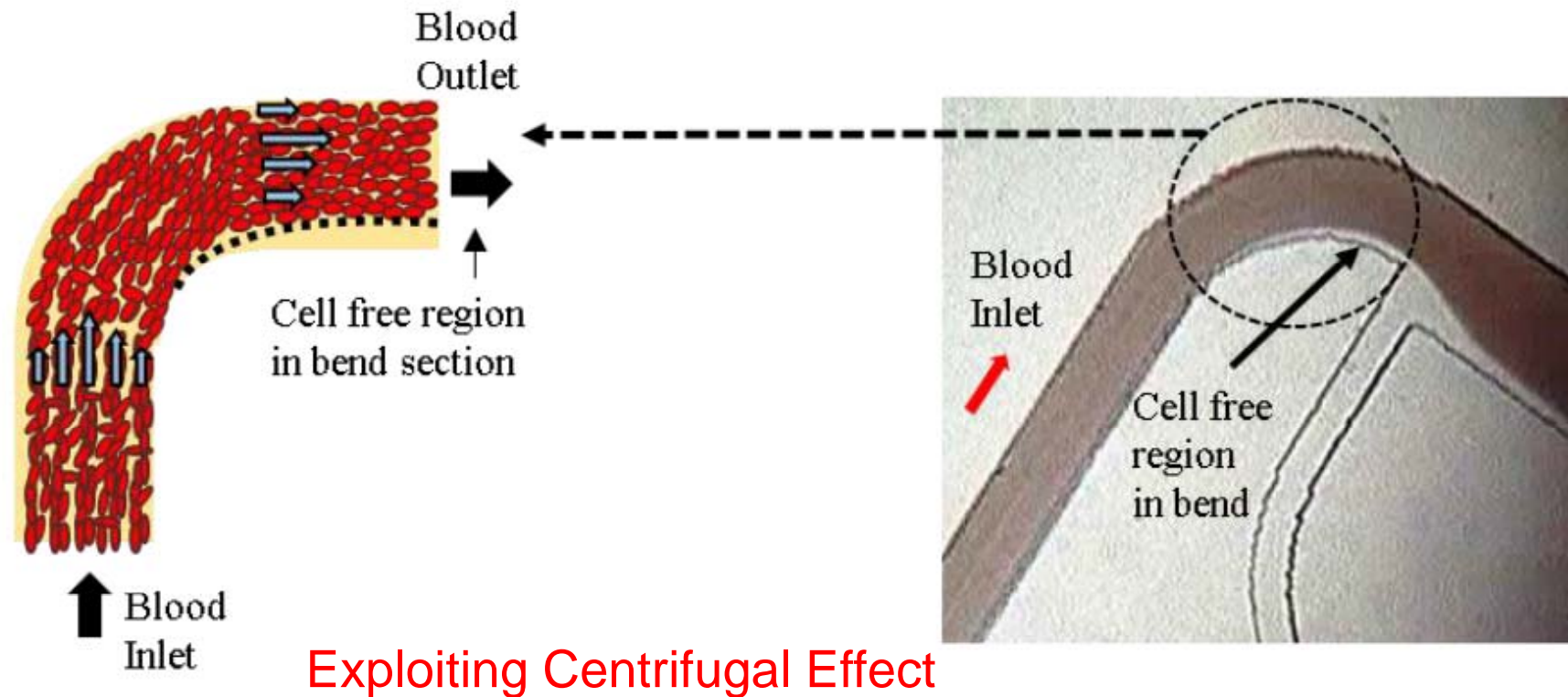


Geometric effect: Constriction-Expansion



Incorporating Constriction-Expansion in a Microchannel

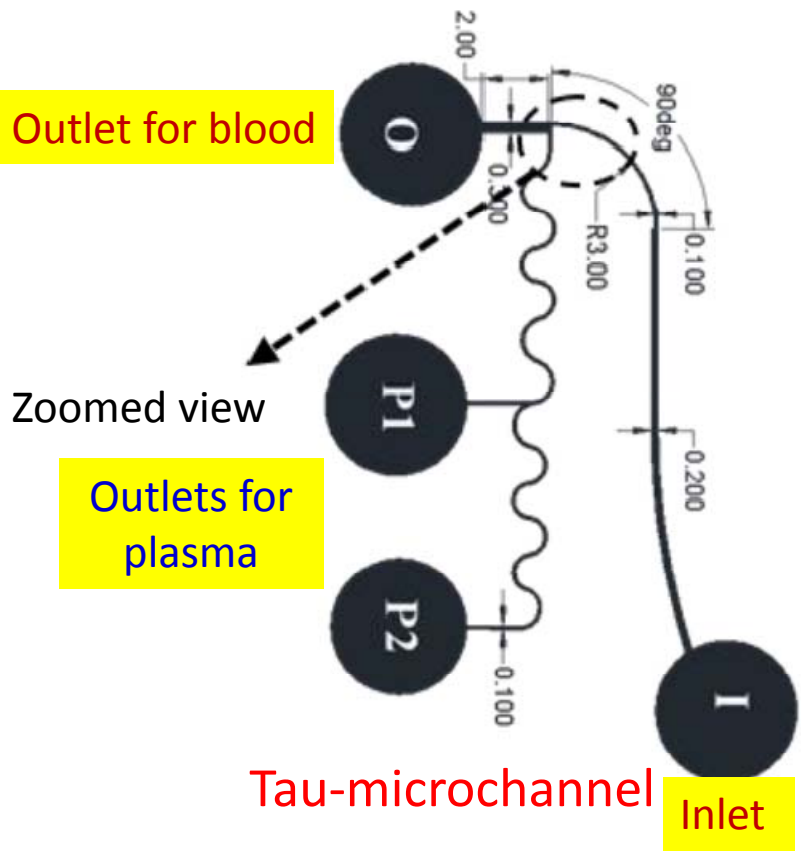
Geometric effect: Centrifugal force



Exploiting Centrifugal Effect

Tripathi, S., Kumar, Y. B. V., Prabhakar, A., Joshi, S. S., & Agrawal, A. (2015). Passive blood plasma separation at the microscale: a review of design principles and microdevices. *Journal of Micromechanics and Microengineering*, 25(8), 083001.

Movie (showing complete separation of plasma)



Outlet for blood

Outlet for plasma

Inlet

Prabhakar et al. (2015) *Microfluidics and Nanofluidics*, 18, 995-1006

Tripathi et al. (2015) *J. Micromechanics and Microengineering*, 25, 084004

Patent pending

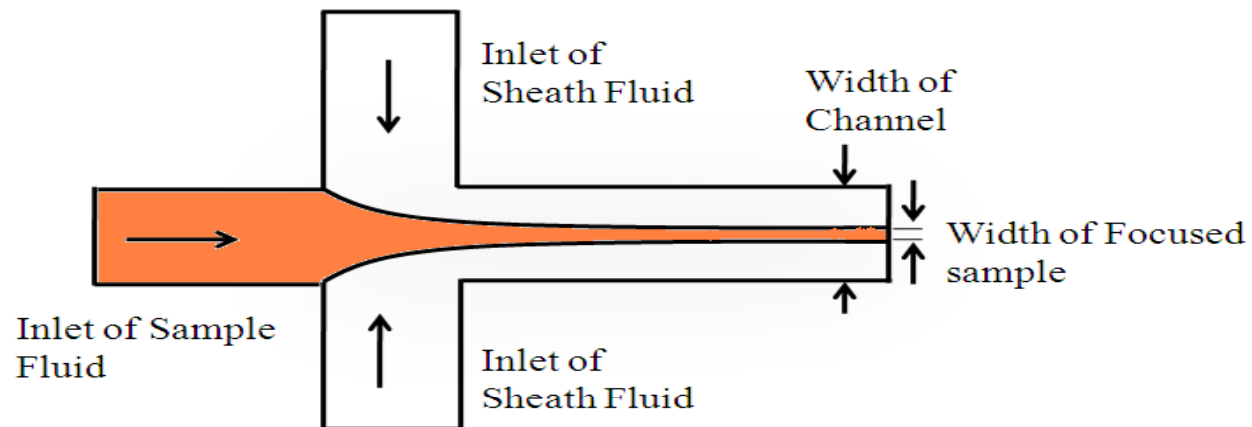
Unique features of our design

- Achieves almost 100% separation efficiency with whole blood
 - Demonstrated in hematocrit of 62% (found in polycythemia – a disease)
- Low separation time (relatively large flow rate: 0.3-0.5 ml/min)
- Elevated dimensions ($> 100 \mu\text{m}$)
 - Avoids problem of clogging!
 - Does not require tight dimensional tolerances
 - Reduces cost of manufacturing
- Biological characterization of plasma shows proteins are unaffected
 - Random-blood glucose test, Hemolysis free, Protein test
- Extensively tested (same microdevice used up to 1 year!)

Device licensed to Embryo Bio-micordevices, Pune

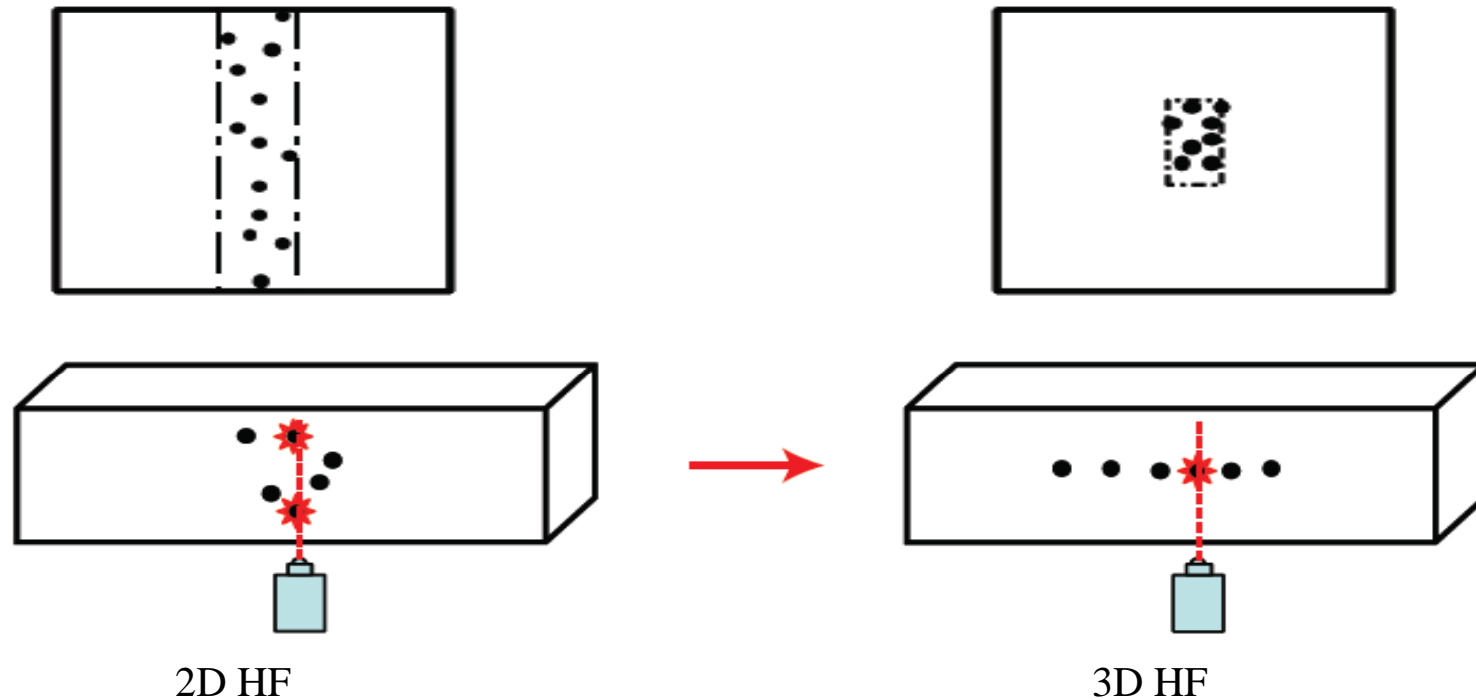
Hydrodynamic focusing microdevice

Hydrodynamic Focusing



Hydrodynamic Flow Focusing: Squeezing of a sample fluid using a sheath fluid. Simple & effective technique for flow focusing and manipulating the sample flow

2D and 3D HF



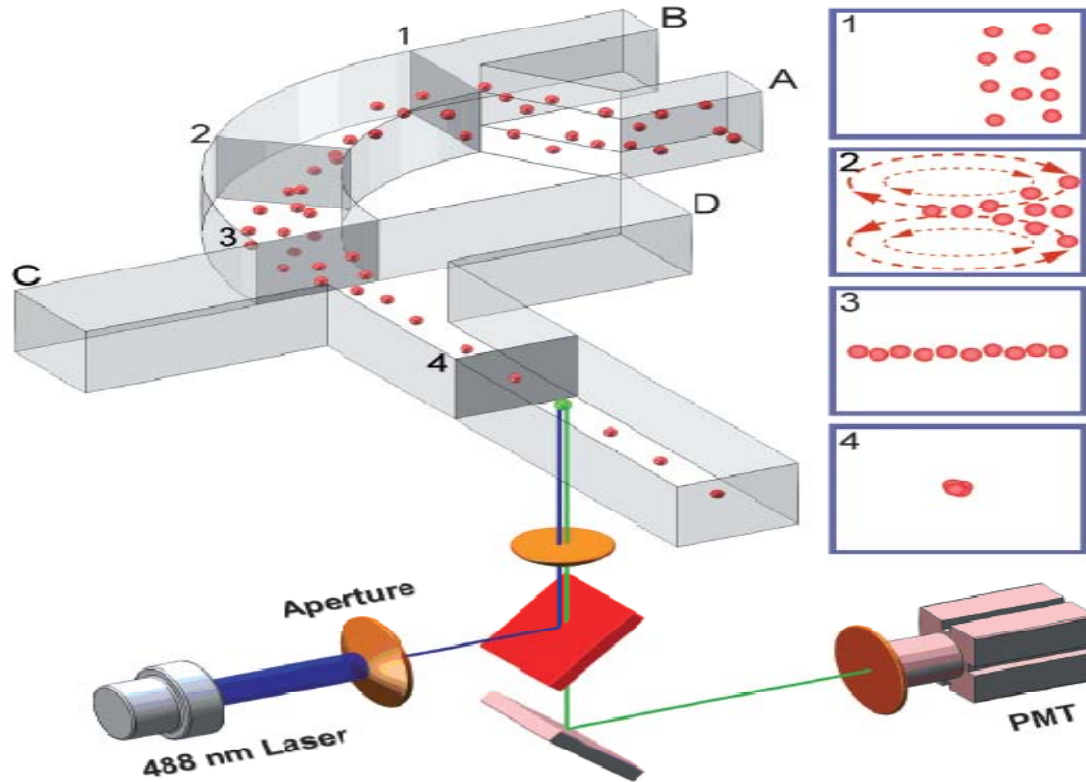
2D HF

3D HF

Disadvantages of 2-D focusing

- 2 or more cells can pass through the interrogation region
- Large cells can clog the microchannel
- Integration with optics
- Less uniform velocities

3D-Hydrodynamic Focusing Microdevice (from literature)



Use of Dean Forces

The device is 75 μm high

The main channel is 100 μm wide and 1 cm long,

Radius of the curve (average of inner and outer portion) is

250 μm .

A=51.9 $\mu\text{l}/\text{min}$, B=337.5 $\mu\text{l}/\text{min}$

C=225.5 $\mu\text{l}/\text{min}$, D=225.5 $\mu\text{l}/\text{min}$

Used LIF

Fluorescent polystyrene 7.32 & 8.32 μm in SDS soln, with De-Ionized Water as sheath

CCD/Side view imaging

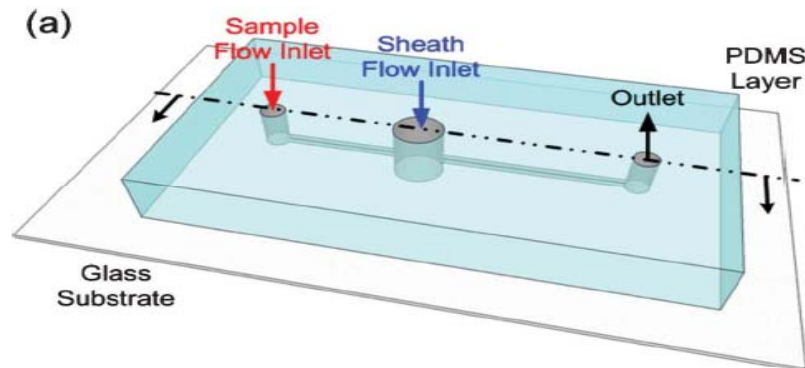
Focused region 14 μm X 12 μm

Rate 1700 cells /sec

Schematic of the device setup and microfluidic drifting mechanism. Inlet A: cells or particles; inlet B: vertical focusing sheath flow; Inlets C and D: horizontal focusing sheath flows. Insets (1–4) on the right show the particle distribution in the cross-sectional planes 1–4 during the 3D hydrodynamic focusing process..

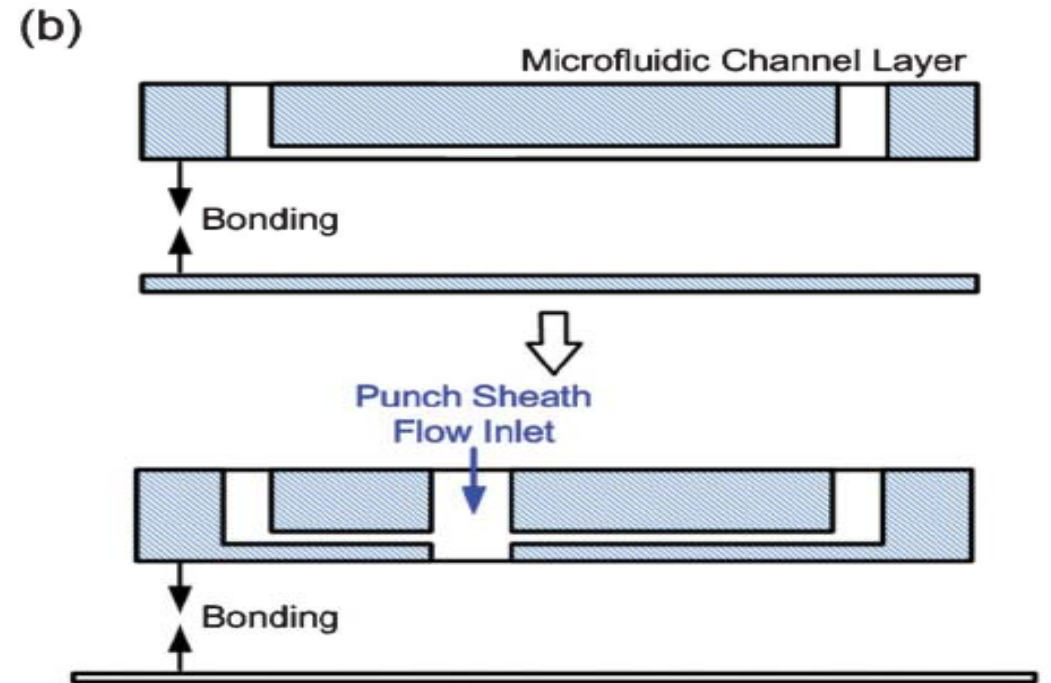
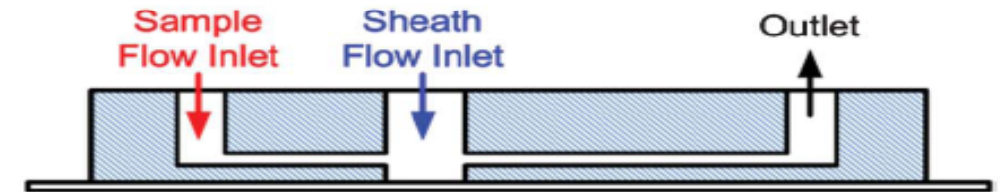
Mao et al, Single-layer planar on-chip flow cytometer using microfluidic drifting based three-dimensional (3D) hydrodynamic focusing, Lab Chip, 9, 1583-1589, 2009

3D Focusing-Single Sheath

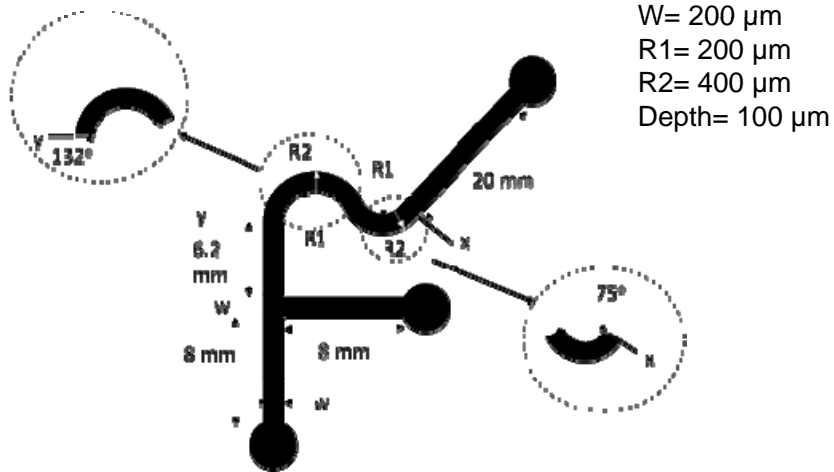


Width = 200 μm , Thickness = 150 μm
Thickness bottom PDMS film = 600 μm
Inlet and outlet hole dia = 1 mm
Sheath dia = 1.5, 2, 3 mm
Water: Sample
Sheath: fluorescein chloride salt
Total flow rate of 100 $\mu\text{l}/\text{min}$
to 600 $\mu\text{l}/\text{min}$, and sheath/sample flow rate ratios of 1 : 1 to 1 : 4 are tested

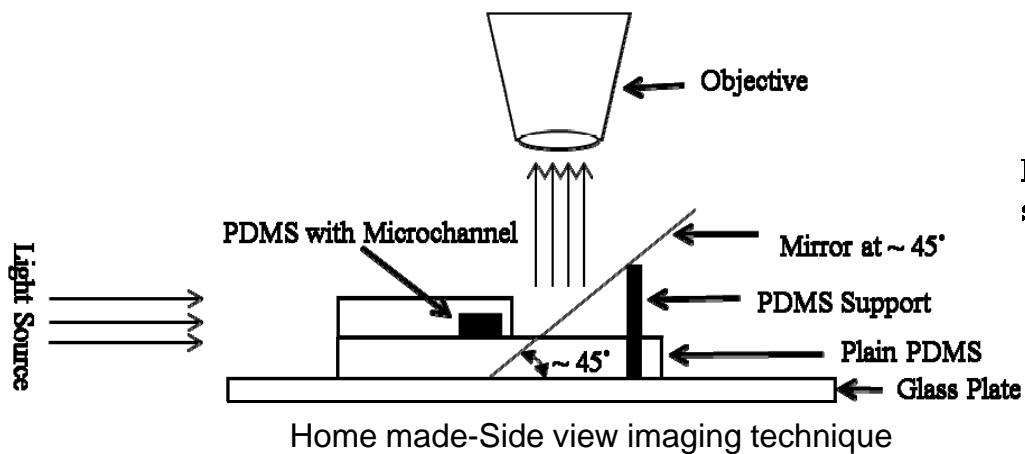
Cross-sectional View:



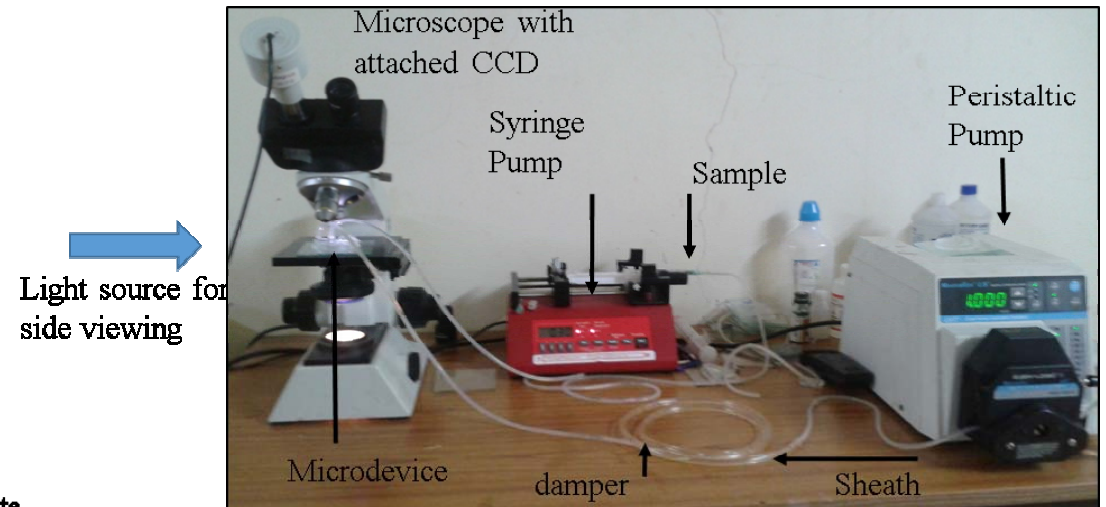
Three-dimensional Hydrodynamic Focusing



Schematic showing geometrical details of the fabricated microdevice



Experiment Details		
Experiment	#1	#2
Sample	FITC Dye and Particles	Blood (Hct 5%)
Sheath	DIW	Saline
Detection	Confocal Microscopy	Microscope and CCD with side view imaging technique

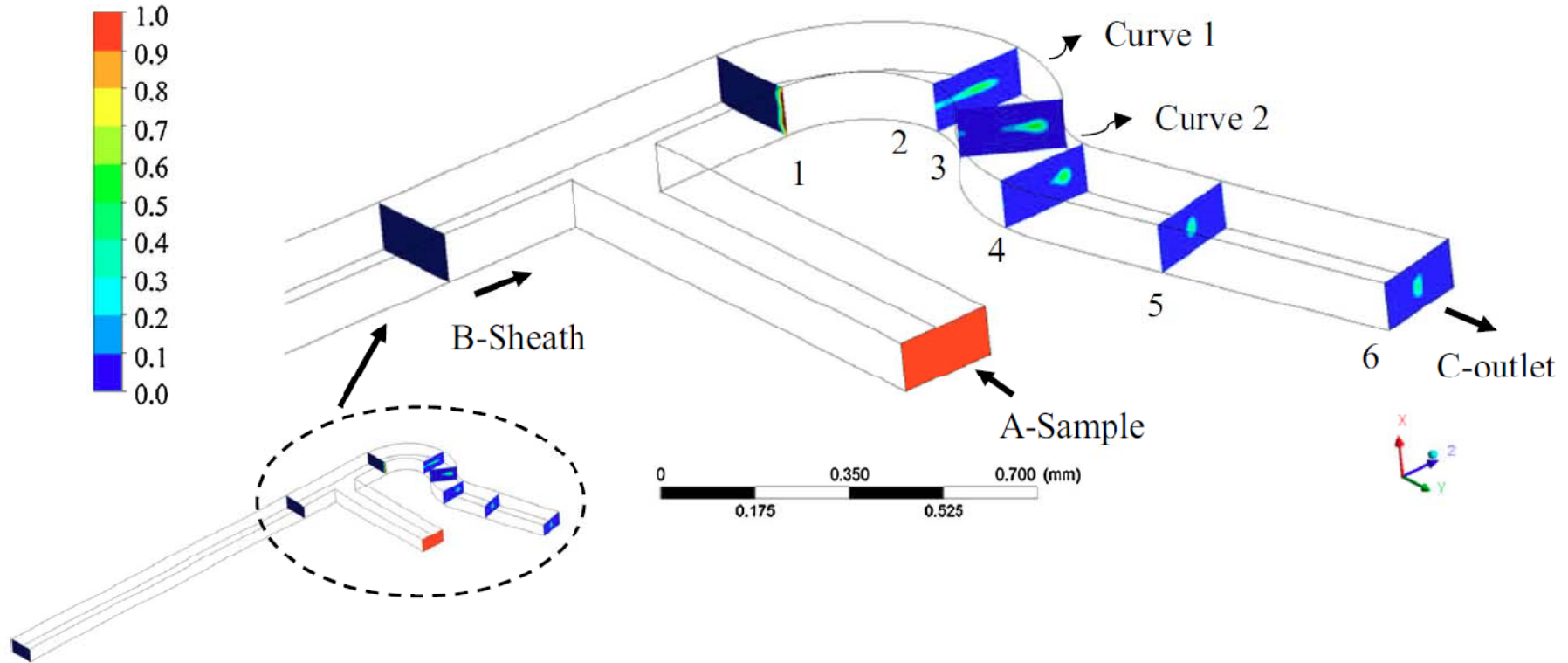


Experimental setup

Three-dimensional Hydrodynamic Focusing (Proposed Device)

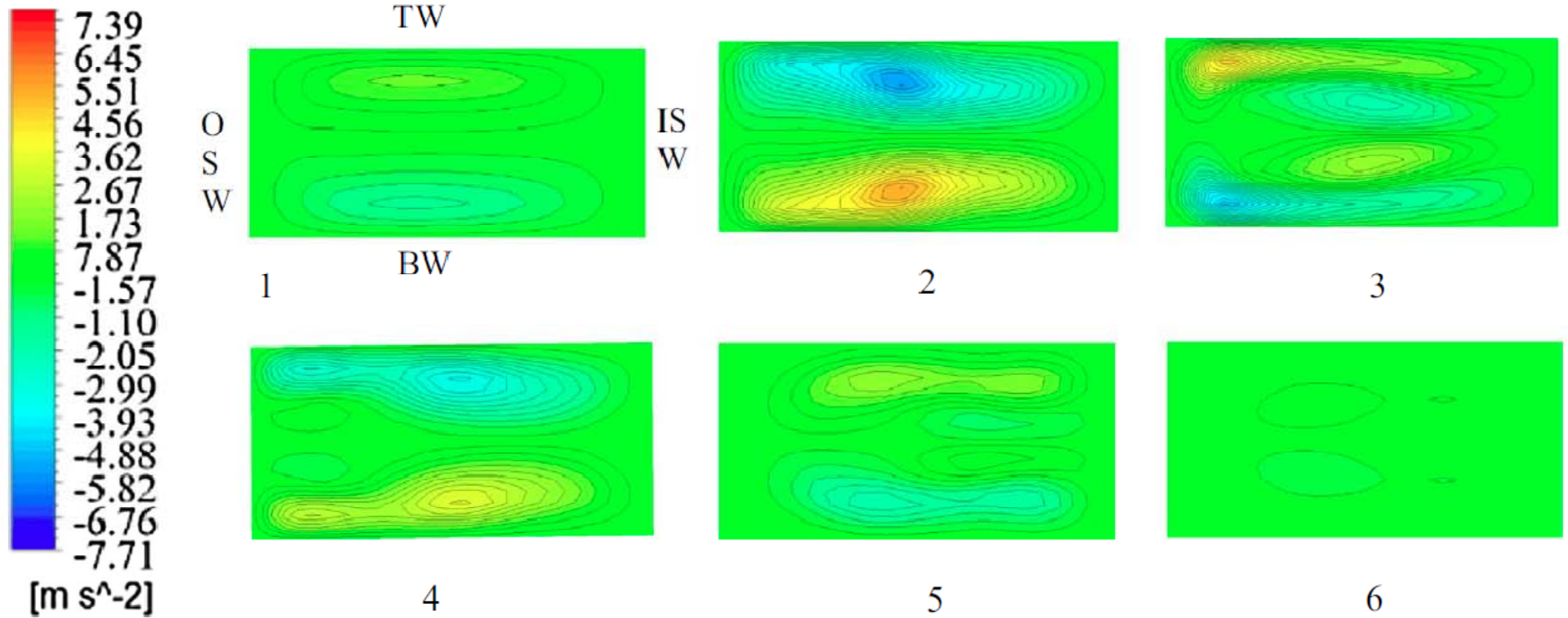
(a)

Sample Volume Fraction



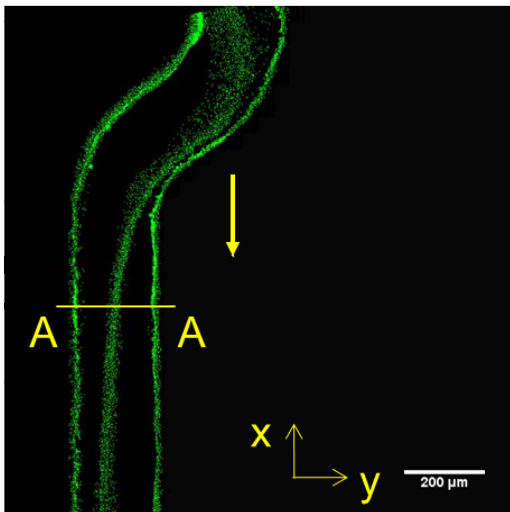
Working of the Microdevice

$Velocity.Helicity \times 10^{-5}$



Cross-sectional view of the microdevice showing formation of Dean's vortices

Experimental Results-FITC Dye and Particles



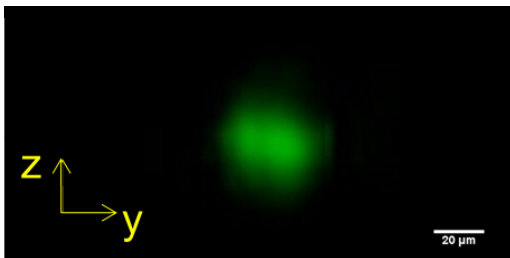
(a)



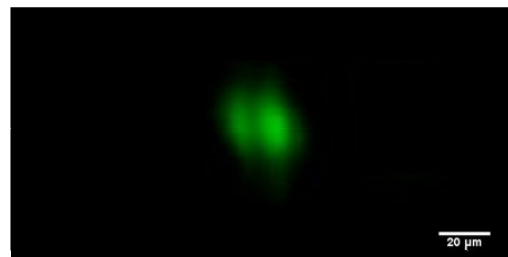
(b)



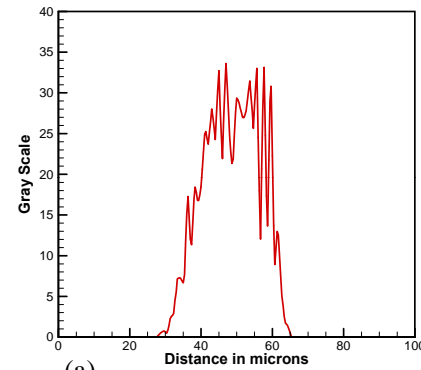
(c)



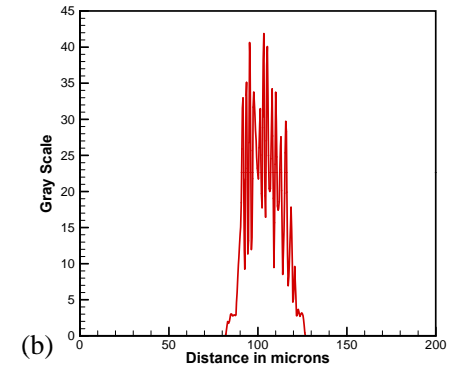
(d)



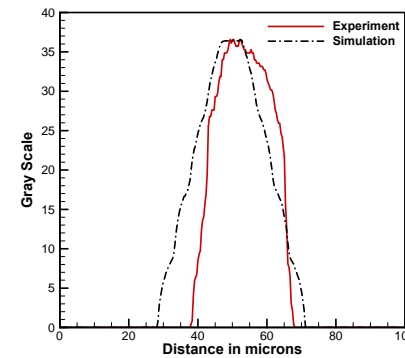
(e)



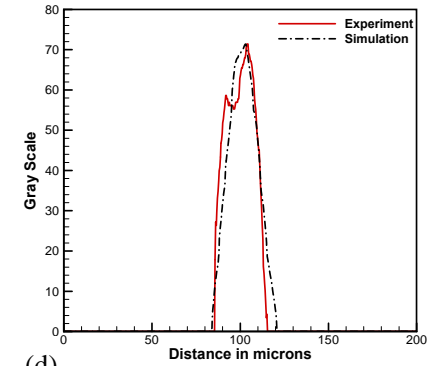
(a)



(b)



(c)

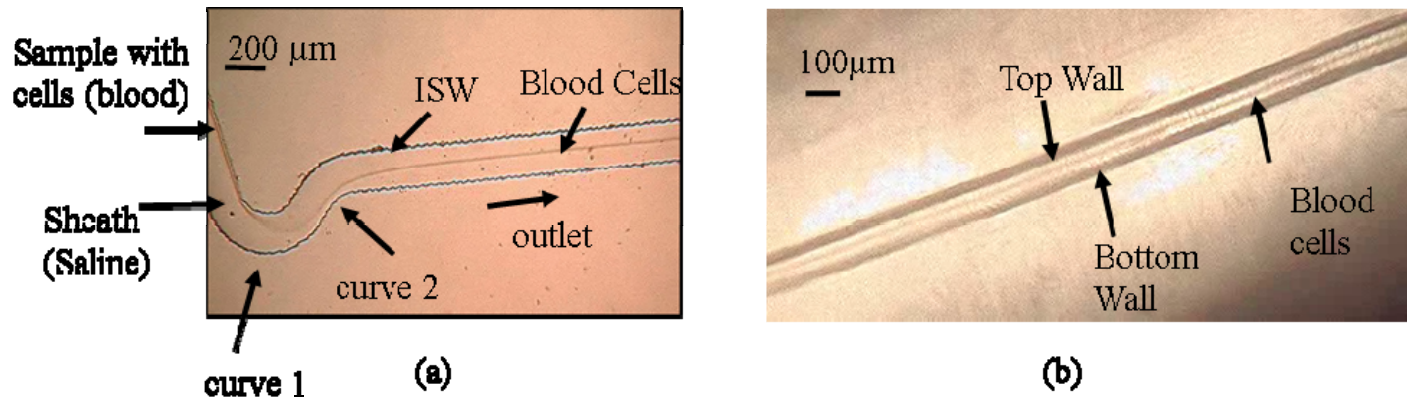


(d)

Intensity profiles for sample and sheath flow rate –
comparison between experiments and simulations

Experimental results using confocal microscopy
Showing three-dimensional hydrodynamic focusing

Experimental Results-Human blood as sample fluid



Experimental result of flow focusing using cells, Sample and sheath flow rate of 0.12 ml/min and 1.8 ml/min respectively (a) Horizontal focusing (b) Vertical focusing of cells

Tripathi, S., Kumar, A., Kmar, B.V., and Agrawal, A., "Three-dimensional hydrodynamic focusing of dye, particles and cells in a microfluidics device by employing two bends of opposite curvature," **Microfluidics and Nanofluidics**, Vol. 20, pp. 1-14, 2016

Device licensed to Embryo Bio-micordeices, Pune

Extension to further
challenging
microdevices ...

		
Nishant Kumar, Project Lead	Prateek Jain, Technology Lead	Apoorva Bedekar, Clinical Applications Lead
		
Sonali Tripathy, Business Lead	Amit Agrawal, PhD, Scientific Advisor	Dr. Vikram Padbidri, Clinical Advisor

 **Embryyo**
LONGITUDE PRIZE
DISCOVERY AWARDS

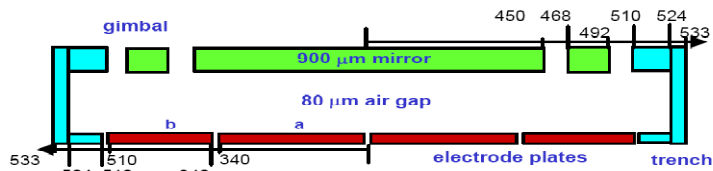
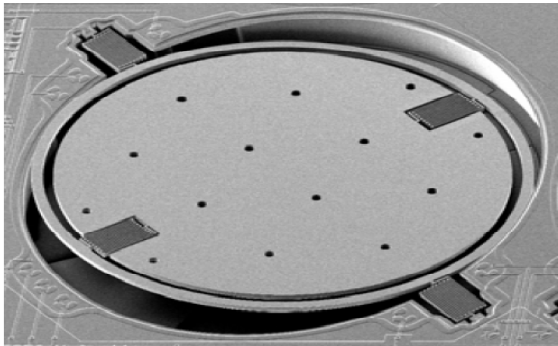
Looking beyond the Navier-Stokes equations

Primary Question

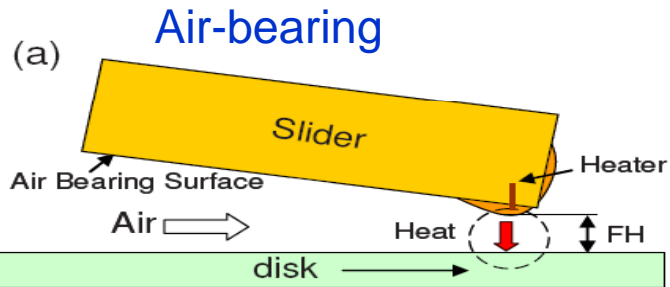
- What is the more general form of the Navier-Stokes equation?
- Recall
 - Navier-Stokes equations represent Conservation of Momentum for a differential fluid element
 - Navier-Stokes equations are 2nd order, non-linear, coupled partial differential equations

Practical Relevance

Flow in MEMS devices



Chu et al., (JMEMS, 2004)

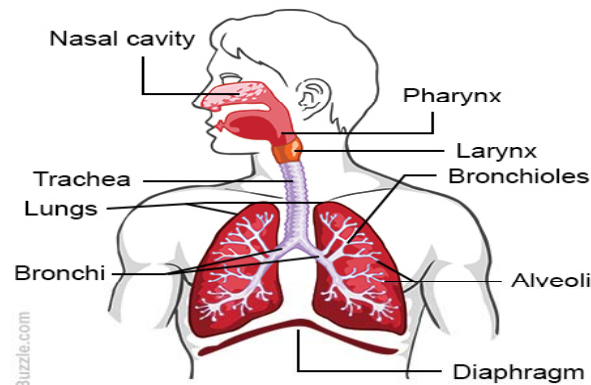


Zhou et al. (PRE, 2010)

Aeration of Soil



Flow in lungs

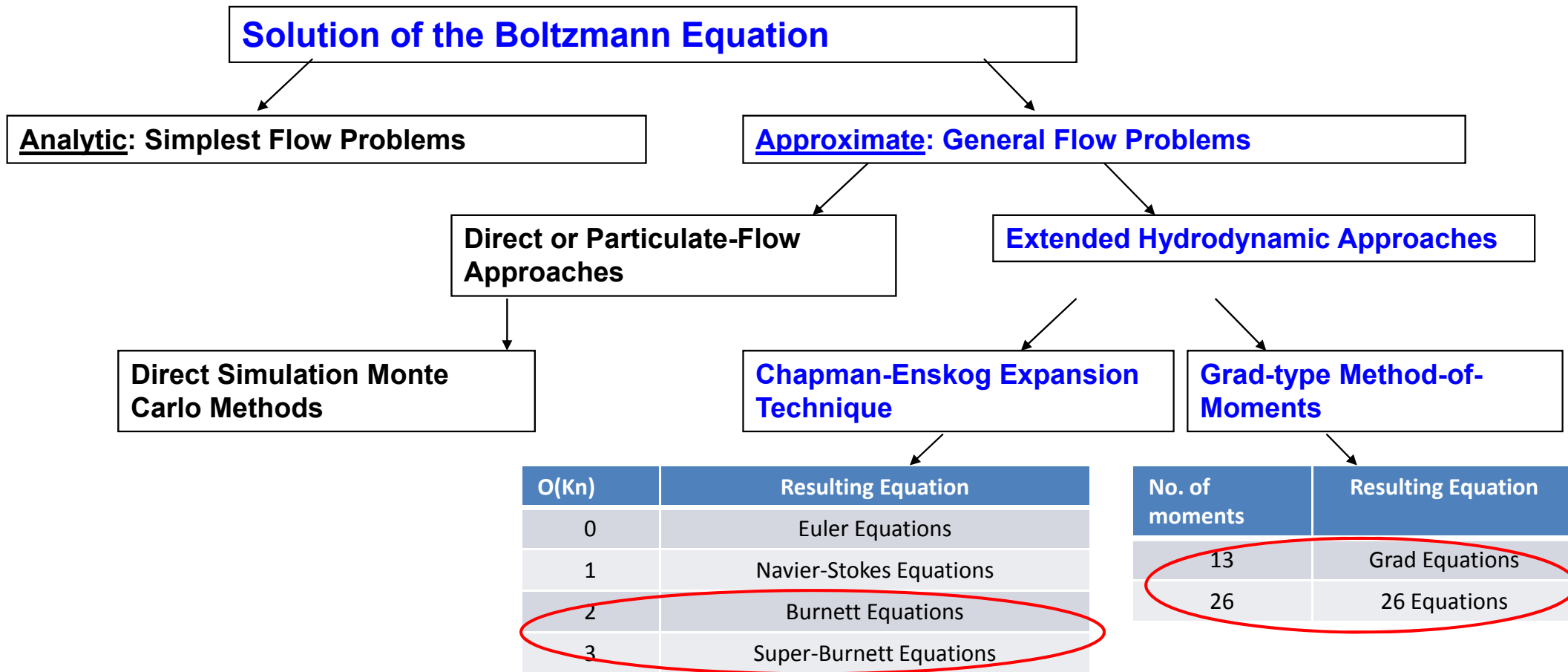


High altitude aircraft flight



Derivation of Hydrodynamic Equations

Adapted from: Balakrishnan, PhD Thesis, Univ. of WSU (1999)



From 'atomistic view' to fluid dynamics

Boltzmann equation:

$$\frac{\partial f}{\partial t} + c_i \frac{\partial f}{\partial x_i} + G_i \frac{\partial f}{\partial c_i} = J(f, f)$$

$$\rho(r, t) = m \int f(r, c, t) dc$$

$$u(r, t) = \frac{1}{n} \int c f(r, c, t) dc$$

$$e(r, t) = \frac{1}{n} \int \frac{m}{2} C^2 f(r, c, t) dc$$

Multiplying by $\psi_i(\mathbf{x}, \mathbf{c}, t) = \{1, \mathbf{c}, C^2\}_i$ and integrating over velocity space, we get the conservation equations.

$$\frac{\partial \rho}{\partial t} + \frac{\partial \rho u_k}{\partial x_k} = 0$$

Continuity equation

$$\rho \frac{\partial u_i}{\partial t} + \rho u_k \frac{\partial u_i}{\partial x_k} + \frac{\partial p}{\partial x_i} + \frac{\partial \sigma_{ik}}{\partial x_k} = \rho G_i,$$

Cauchy's equation of motion

$$\rho \frac{\partial \epsilon}{\partial t} + \rho u_k \frac{\partial \epsilon}{\partial x_k} + p \frac{\partial u_k}{\partial x_k} + \frac{\partial q_k}{\partial x_k} + \sigma_{ij} \frac{\partial u_i}{\partial x_j} = 0,$$

Energy equation

System of equations is not closed.

The Chapman-Enskog method

Perturbative method based on an expansion in terms of Kn,

$$f = f^{(0)} + \epsilon f^{(1)} + \epsilon^2 f^{(2)} + \epsilon^3 f^{(3)} + \dots$$

$$\sigma_{ij} = m \int C_{<i} C_{j>} f d\mathbf{c}, \quad q_i = \frac{m}{2} \int C^2 C_i f d\mathbf{c}$$

$$\sigma_{ij} = \sigma_{ij}^{(0)} + \epsilon \sigma_{ij}^{(1)} + \epsilon^2 \sigma_{ij}^{(2)} + \epsilon^3 \sigma_{ij}^{(3)} + \dots,$$

$$q_i = q_i^{(0)} + \epsilon q_i^{(1)} + \epsilon^2 q_i^{(2)} + \epsilon^3 q_i^{(3)} + \dots$$

In increasing order of Knudsen number,

- $O(\text{Kn}^0)$: Euler
- $O(\text{Kn}^1)$: Navier-Stokes-Fourier
- $O(\text{Kn}^2)$: Burnett
- $O(\text{Kn}^3)$: Super-Burnett

Burnett (1935) obtained the distribution function to second order.

Burnett stress and heat flux

Burnett

$$\sigma_{ij}^{(2)} = \frac{\mu^2}{p} \left[\overline{\omega}_1 \frac{\partial v_k}{\partial x_k} S_{ij} - \overline{\omega}_2 \left(\frac{\partial}{\partial x_{\langle i}} \left[\frac{1}{\rho} \frac{\partial p}{\partial x_{j \rangle}} \right] + \frac{\partial v_k}{\partial x_{\langle i}} \frac{\partial v_{j \rangle}}{\partial x_k} + 2 \frac{\partial v_k}{\partial x_{\langle i}} S_{j \rangle k} \right) \right. \\ \left. + \overline{\omega}_3 \frac{\partial^2 \theta}{\partial x_{\langle i} \partial x_{j \rangle}} + \overline{\omega}_4 \frac{\partial \theta}{\partial x_{\langle i}} \frac{\partial \ln p}{\partial x_{j \rangle}} + \overline{\omega}_5 \frac{1}{\theta} \frac{\partial \theta}{\partial x_{\langle i}} \frac{\partial \theta}{\partial x_{j \rangle}} + \overline{\omega}_6 S_{k \langle i} S_{j \rangle k} \right]$$

$$q_i^{(2)} = \frac{\mu^2}{\rho} \left[\theta_1 \frac{\partial v_k}{\partial x_k} \frac{\partial \ln \theta}{\partial x_i} - \theta_2 \left(\frac{2}{3} \frac{\partial^2 v_k}{\partial x_k \partial x_i} + \frac{2}{3} \frac{\partial v_k}{\partial x_k} \frac{\partial \ln \theta}{\partial x_i} + 2 \frac{\partial v_k}{\partial x_i} \frac{\partial \ln \theta}{\partial x_k} \right) \right. \\ \left. + \theta_3 S_{ik} \frac{\partial \ln p}{\partial x_k} + \theta_4 \frac{\partial S_{ik}}{\partial x_k} + 3\theta_5 S_{ik} \frac{\partial \ln \theta}{\partial x_k} \right]$$

Super-Burnett

Computation extremely complicated, hence three dimensional equations are still not known

Burnett Stress term in Cylindrical Coordinates ($\sigma_{r\theta}$)

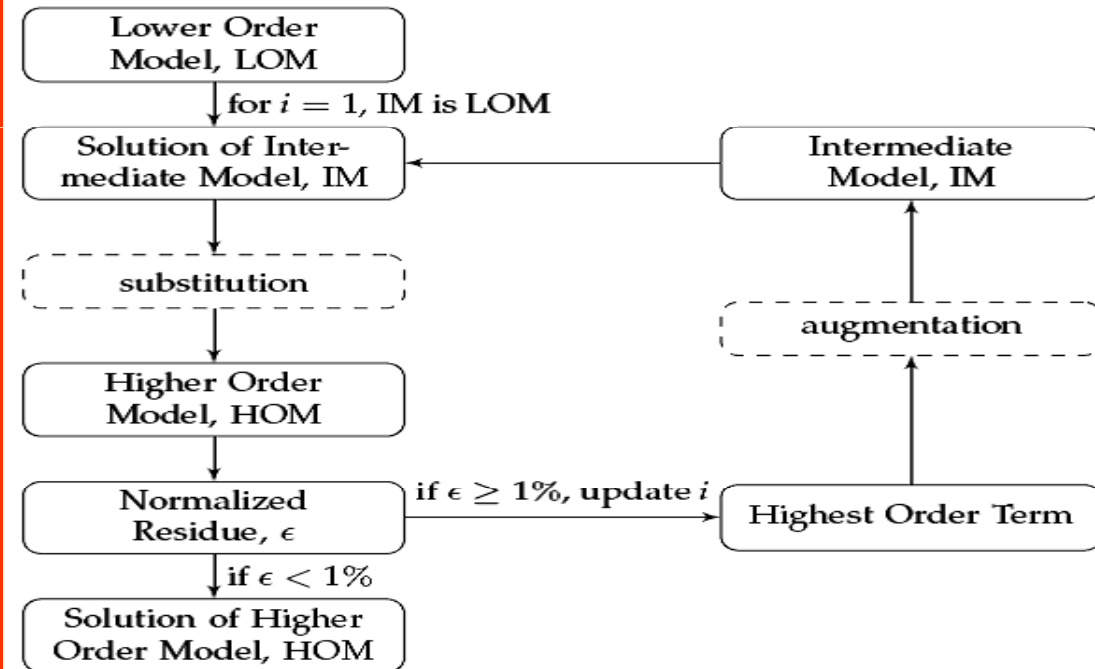
$$\begin{aligned}
 \sigma_{r\theta}^B = \sigma_{\theta r}^B = & \frac{\mu^2}{p} \left[- \left(\frac{\omega_1}{2} - \frac{5\omega_2}{3} + \frac{\omega_6}{6} \right) \left(\frac{v}{r} \frac{\partial u}{\partial r} \right) + \left(\frac{\omega_1}{2} - \frac{2\omega_2}{3} + \frac{\omega_6}{6} \right) \left(\frac{u}{r^2} \frac{\partial u}{\partial \theta} \right) \right. \\
 & - \left(\frac{\omega_1}{2} - \frac{2\omega_2}{3} - \frac{\omega_6}{6} \right) \left(\frac{uv}{r^2} \right) + \left(\frac{\omega_1}{2} - \frac{5\omega_2}{3} + \frac{\omega_6}{6} \right) \left(\frac{u}{r} \frac{\partial v}{\partial r} \right) \\
 & - \left(\frac{\omega_1}{2} - \frac{2\omega_2}{3} + \frac{\omega_6}{6} \right) \left(\frac{v}{r^2} \frac{\partial v}{\partial \theta} \right) - \left(\frac{\omega_1}{2} + \frac{\omega_2}{3} - \frac{\omega_6}{3} \right) \left(\frac{v}{r} \frac{\partial w}{\partial z} \right) \\
 & + \left(\frac{\omega_1}{2} + \frac{\omega_2}{3} - \frac{\omega_6}{3} \right) \left(\frac{1}{r} \frac{\partial u}{\partial \theta} \frac{\partial w}{\partial z} \right) + \left(\frac{\omega_1}{2} - \frac{5\omega_2}{3} + \frac{\omega_6}{6} \right) \left(\frac{1}{r} \frac{\partial u}{\partial r} \frac{\partial u}{\partial \theta} \right) \\
 & + \left(\frac{\omega_1}{2} + \frac{\omega_2}{3} - \frac{\omega_6}{3} \right) \left(\frac{\partial v}{\partial r} \frac{\partial w}{\partial z} \right) + \left(\frac{\omega_1}{2} - \frac{2\omega_2}{3} + \frac{\omega_6}{6} \right) \left(\frac{\partial u}{\partial r} \frac{\partial v}{\partial r} \right) \\
 & + \left(\frac{\omega_1}{2} - \frac{2\omega_2}{3} + \frac{\omega_6}{6} \right) \left(\frac{1}{r^2} \frac{\partial u}{\partial \theta} \frac{\partial v}{\partial \theta} \right) + \left(\frac{\omega_1}{2} - \frac{5\omega_2}{3} + \frac{\omega_6}{6} \right) \left(\frac{1}{r} \frac{\partial v}{\partial r} \frac{\partial v}{\partial \theta} \right) \\
 & - \left(\omega_2 - \frac{\omega_6}{4} \right) \left(\frac{\partial v}{\partial z} \frac{\partial w}{\partial r} \right) - \left(\omega_2 - \frac{\omega_6}{4} \right) \left(\frac{1}{r} \frac{\partial u}{\partial z} \frac{\partial w}{\partial \theta} \right) - \left(\omega_2 - \frac{\omega_6}{4} \right) \left(\frac{1}{r} \frac{\partial w}{\partial r} \frac{\partial w}{\partial \theta} \right) \\
 & + \omega_3 \frac{R}{r} \frac{\partial^2 T}{\partial r \partial \theta} - \omega_3 \frac{R}{r^2} \frac{\partial T}{\partial \theta} + \frac{\omega_4}{2} \frac{R}{r} \frac{1}{p} \frac{\partial p}{\partial \theta} \frac{\partial T}{\partial r} + \frac{\omega_4}{2} \frac{1}{r} \frac{R}{p} \frac{\partial p}{\partial r} \frac{\partial T}{\partial \theta} \\
 & + \omega_5 \frac{1}{T} \frac{R}{r} \frac{\partial T}{\partial r} \frac{\partial T}{\partial \theta} + \frac{\omega_6}{4} \frac{\partial u}{\partial z} \frac{\partial v}{\partial z} + \omega_2 \frac{1}{r^2} \frac{1}{\rho} \frac{\partial p}{\partial \theta} - \omega_2 \frac{1}{r} \frac{1}{\rho} \frac{\partial^2 p}{\partial r \partial \theta} + \frac{\omega_2}{2} \frac{1}{r} \frac{1}{\rho^2} \frac{\partial p}{\partial \theta} \frac{\partial \rho}{\partial r} + \frac{\omega_2}{2} \frac{1}{r} \frac{1}{\rho^2} \frac{\partial p}{\partial r} \frac{\partial \rho}{\partial \theta} \left. \right]
 \end{aligned}$$

Just one of the stress terms!

Question: Is it possible to obtain an analytical solution of the Burnett equations?

Proposed Approach to Solve Burnett Equations

- Start with solution of Navier-Stokes equations
- Substitute in Burnett equations
 - evaluate order of magnitude of additional terms
- Identify highest order term
 - augment governing equation with this additional term
- Re-solve the resulting equations
- Repeat above steps, till convergence achieved



Note: Requirement of additional boundary condition deferred till third-order term gets added in the governing equation!

Singh and Agrawal, Journal of Fluid Mechanics, 2014

Solution of Burnett Equation for plane Poiseuille Flow

▶ Streamwise Velocity

$$\square \quad u(x, y) = \left(\frac{\text{Re} \mu R T}{p D_h} \right) \frac{\left[\frac{y}{H} - \left(\frac{y}{H} \right)^2 + 2C_1 \text{Kn} + 8C_2 \text{Kn}^2 \right]}{\left(\frac{1}{6} + 2C_1 \text{Kn} + 8C_2 \text{Kn}^2 \right)}$$

▶ Cross-Stream Velocity

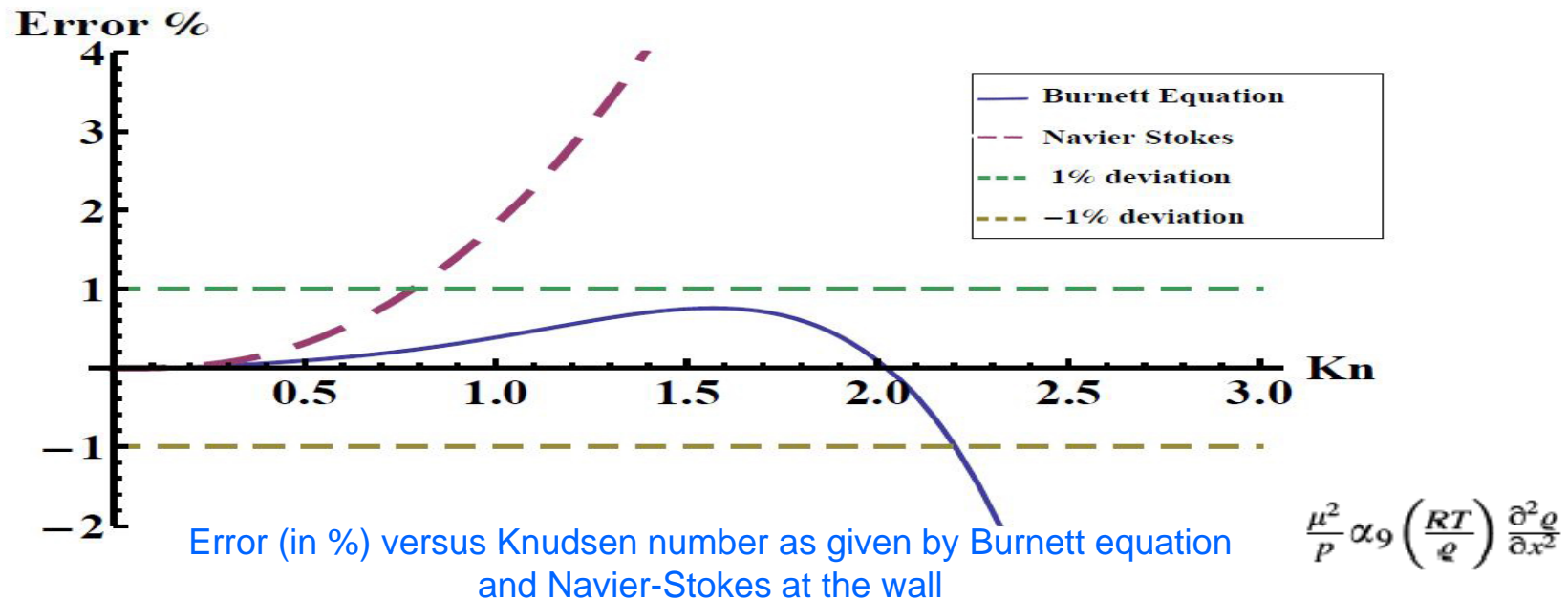
$$\square \quad v(x, y) = \frac{(12C_1 \text{Kn} + 96C_2 \text{Kn}^2)}{(1 + 12C_1 \text{Kn} + 48C_2 \text{Kn}^2)} \left(\frac{\text{Re} \mu R T}{D_h} \right) \left(\frac{1}{p^2} \right) \left(\frac{dp}{dx} \right) \times \left\{ y \left[1 - \frac{\frac{3y}{H} - 2\left(\frac{y}{H}\right)^2 + 12C_1 \text{Kn} + 48C_2 \text{Kn}^2}{(1 + 12C_1 \text{Kn} + 48C_2 \text{Kn}^2)} \right] \right\}$$

▶ Pressure

$$\square \quad \left(\frac{p}{p_o} \right)^2 - 1 + \text{Re}^2 \omega \frac{\mu^2 R T}{(D_h^2 p_o^2)} \left\{ 12C_1 \text{Kn}_o \left(\frac{p_o}{p} - 1 \right) + 24C_2 \text{Kn}_o^2 \left[\left(\frac{p_o}{p} \right)^2 - 1 \right] + \log \left(\frac{p_o}{p} \right) \right\} + 96C_2 \text{Kn}_o^2 \log \left(\frac{p}{p_o} \right) + 24C_1 \text{Kn}_o \left(\frac{p}{p_o} - 1 \right) = 96 \text{Re} \frac{\mu^2 R T}{(D_h^2 p_o^2)} \frac{(x_o - x)}{D_h}$$

Validation of Proposed Solution

Normalized error upon substituting the solution in governing equation is evaluated



Normalized error less than 1% till $Kn = 2.2$

Solution satisfies governing equation (and boundary conditions)

N. Singh, N. Dongari, A. Agrawal (2014) Analytical solution of plane Poiseuille flow within Burnett hydrodynamics, *Microfluidics and Nanofluidics*, Vol. 16, pp. 403-412

Critiques against Burnett equations

- Requires additional boundary conditions
 - Due to presence of the higher order derivatives
 - Additional boundary conditions are generally not available
- The convergence properties of the Chapman-Enskog series are not known.
- The equations suffer from instabilities in transient processes and from unphysical oscillations in steady state processes (Bobylev's instability)
- So far, there is *no proof that the Burnett equations follow positive definite entropy production*

Variants of Burnett equations: BGK-Burnett, Augmented Burnett, simplified Burnett, Dadzie-Burnett

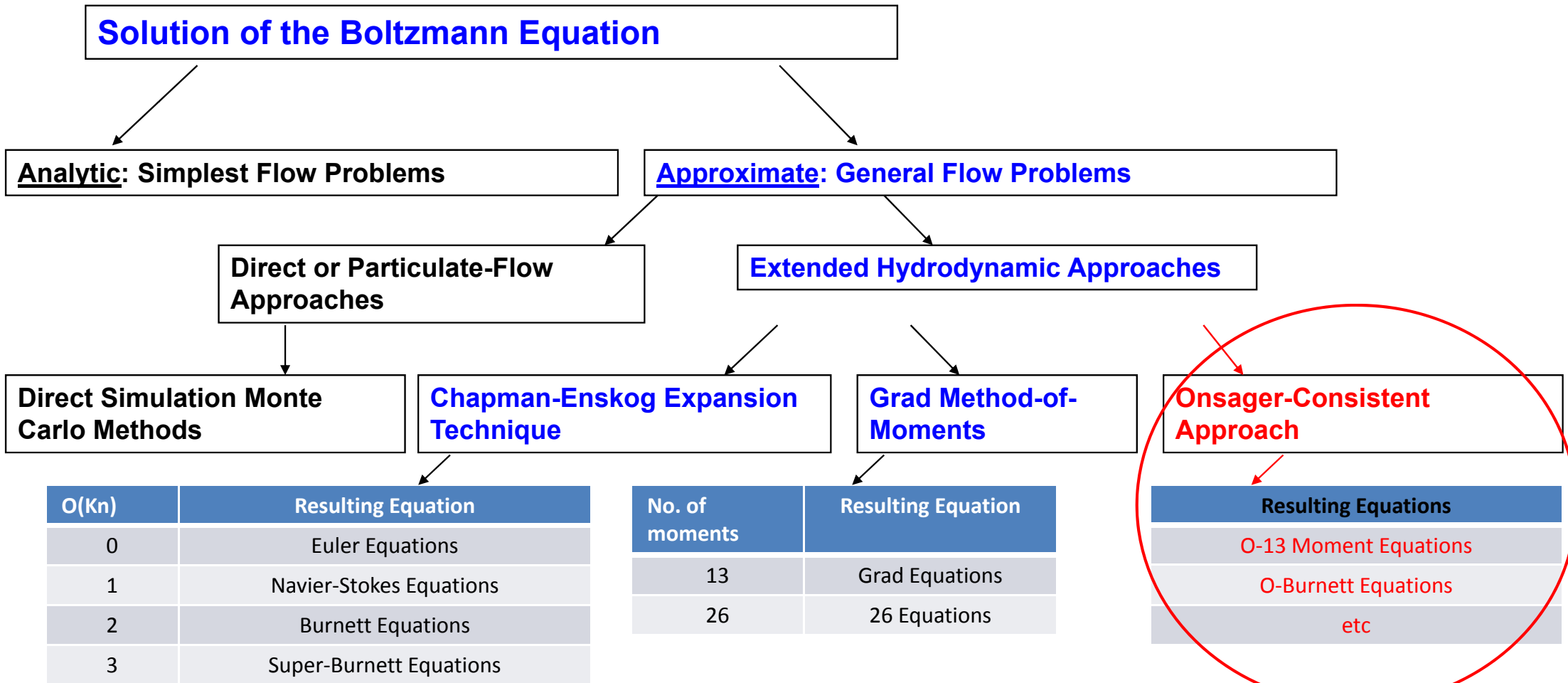
All these variants are inconsistent!

In general, Burnett and Grad's equations do not perform well at high Knudsen numbers!

Ref: Agarwal et al., PoF (2001); Garcia-Colin et al., Physics Reports (2008); Dadzie, JFM (2012)

Derivation of (Better?) Higher Order Moment Equations

Our Approach



Proposed distribution function

Phase density function casted in terms of thermodynamic forces X_i and fluxes Y_i

Satisfies Onsager's symmetry principle

$$f' = f_0 - (\Upsilon_\tau : X_\tau + \Upsilon_q \cdot X_q + (\Upsilon'_{\tau\tau} \odot X_\tau) : X_\tau + (\Upsilon'_{qq} \odot X_q) \cdot X_q)$$

Final form of distribution function satisfies

- Linearized Boltzmann equation
- Collision invariance property
- Onsager's symmetry principle

Therefore, consistent with principles of non-equilibrium thermodynamics

Note, no reference to Knudsen number in the derivation

- Expect to capture relatively strong non-equilibrium effects in slip and transition regimes

A. Mahendra, Meshless method for slip flows, *Ph.D. thesis*, Homi Bhabha National Institute, Mumbai (2011)

N. Singh and A. Agrawal, Onsager's principle consistent 13-moment transport equations, *Physical Review E* **93**, 063111 (2016)

Derivation of Onsager-Burnett Equations

$$\frac{\partial \rho}{\partial t} + \frac{\partial \rho u_k}{\partial x_k} = 0$$

$$\rho \frac{\partial u_i}{\partial t} + \rho u_k \frac{\partial u_i}{\partial x_k} + \frac{\partial p}{\partial x_i} + \frac{\partial \sigma_{ik}}{\partial x_k} = \rho G_i,$$

$$\rho \frac{\partial \epsilon}{\partial t} + \rho u_k \frac{\partial \epsilon}{\partial x_k} + p \frac{\partial u_k}{\partial x_k} + \frac{\partial q_k}{\partial x_k} + \sigma_{ij} \frac{\partial u_i}{\partial x_j} = 0,$$

Utilize the Onsager-consistent distribution function to evaluate σ_{ij} and q_i and obtain Burnett-type equations.

Proposed Onsager-Burnett equations

Euler/NSF/O-Burnett

$$\frac{\partial \rho}{\partial t} + \frac{\partial \rho u_k}{\partial x_k} = 0, \quad \text{Continuity equation}$$

$$\rho \frac{\partial u_i}{\partial t} + \rho u_k \frac{\partial u_i}{\partial x_k} + \frac{\partial p}{\partial x_i} + \left[\frac{\partial \sigma_{ik}}{\partial x_k} \right] = \rho G_i, \quad \text{Cauchy's equation of motion}$$

$$\rho \frac{\partial \epsilon}{\partial t} + \rho u_k \frac{\partial \epsilon}{\partial x_k} + p \frac{\partial u_k}{\partial x_k} + \left[\frac{\partial q_k}{\partial x_k} + \sigma_{ij} \frac{\partial u_i}{\partial x_j} \right] = 0, \quad \text{Energy equation}$$

Constitutive relationships: [Singh et al., Derivation of stable Burnett equations for rarefied gas flows, PRE \(2017\)](#)

$$\begin{aligned} \sigma_{xx} = \sigma_{xx}^{NS} + \sigma_{xx}^B = & \left[\mu \left(\delta_1 \frac{\partial u}{\partial x} + \delta_2 \frac{\partial v}{\partial y} + \delta_2 \frac{\partial w}{\partial z} \right) \right] + 4 \frac{\mu^2 \beta}{\rho} \left[\alpha_1 \left(\frac{\partial u}{\partial x} \right)^2 + \alpha_2 \left(\frac{\partial u}{\partial y} \right)^2 + \alpha_3 \left(\frac{\partial u}{\partial z} \right)^2 \right. \\ & + \alpha_4 \frac{\partial u}{\partial y} \frac{\partial v}{\partial x} + \alpha_5 \frac{\partial u}{\partial z} \frac{\partial w}{\partial x} + \alpha_6 \left(\frac{\partial w}{\partial x} \right)^2 + \alpha_7 \left(\frac{\partial v}{\partial x} \right)^2 + \alpha_8 \frac{\partial u}{\partial x} \frac{\partial v}{\partial y} + \alpha_9 \left(\frac{\partial v}{\partial y} \right)^2 + \alpha_{10} \left(\frac{\partial w}{\partial z} \right)^2 \\ & \left. + \alpha_{11} \frac{\partial v}{\partial y} \frac{\partial w}{\partial z} + \alpha_{12} \frac{\partial u}{\partial x} \frac{\partial w}{\partial z} + \alpha_{13} \frac{\partial v}{\partial z} \frac{\partial w}{\partial y} + \alpha_{14} \left(\frac{\partial w}{\partial y} \right)^2 + \alpha_{15} \left(\frac{\partial v}{\partial z} \right)^2 \right], \end{aligned}$$

$$\begin{aligned} \sigma_{xy} = \sigma_{xy}^{NS} + \sigma_{xy}^B = & \left[\mu \delta_3 \frac{\partial u}{\partial y} + \mu \delta_3 \frac{\partial v}{\partial x} \right] + 4 \frac{\mu^2 \beta}{\rho} \left[\beta_1 \frac{\partial u}{\partial x} \frac{\partial u}{\partial y} + \beta_2 \frac{\partial v}{\partial x} \frac{\partial v}{\partial y} + \beta_3 \frac{\partial u}{\partial z} \frac{\partial v}{\partial z} + \beta_4 \frac{\partial u}{\partial x} \frac{\partial v}{\partial x} \right. \\ & \left. + \beta_5 \frac{\partial u}{\partial y} \frac{\partial v}{\partial y} + \beta_6 \frac{\partial w}{\partial x} \frac{\partial w}{\partial y} + \beta_7 \frac{\partial v}{\partial z} \frac{\partial w}{\partial x} + \beta_8 \frac{\partial u}{\partial z} \frac{\partial w}{\partial y} + \beta_9 \frac{\partial u}{\partial y} \frac{\partial w}{\partial z} + \beta_{10} \frac{\partial v}{\partial x} \frac{\partial w}{\partial z} \right], \end{aligned}$$

Proposed Onsager-Burnett equations

Euler/NSF/O-Burnett

$$\begin{aligned}
 q_x = q_x^{NS} + q_x^B = & \delta_4 \kappa \frac{1}{2R\beta^2} \frac{\partial \beta}{\partial x} + 4 \frac{\mu^2 \beta}{\rho} \left[\gamma_1 \frac{1}{\beta} \frac{\partial g}{\partial x} \frac{\partial u}{\partial x} + \gamma_2 \frac{1}{\beta^2} \frac{\partial \beta}{\partial x} \frac{\partial v}{\partial y} + \gamma_3 \frac{1}{\beta^2} \frac{\partial \beta}{\partial x} \frac{\partial w}{\partial z} + \gamma_4 \frac{1}{\beta} \frac{\partial g}{\partial y} \frac{\partial u}{\partial y} \right. \\
 & + \gamma_5 \frac{1}{\beta} \frac{\partial g}{\partial y} \frac{\partial v}{\partial x} + \gamma_6 \frac{1}{\beta} \frac{\partial g}{\partial z} \frac{\partial w}{\partial x} + \gamma_7 \frac{1}{\beta^2} \frac{\partial \beta}{\partial x} \frac{\partial u}{\partial x} + \gamma_8 \frac{1}{\beta^2} \frac{\partial \beta}{\partial y} \frac{\partial u}{\partial y} + \gamma_9 \frac{1}{\beta^2} \frac{\partial \beta}{\partial z} \frac{\partial u}{\partial z} + \gamma_{10} \frac{1}{\beta^2} \frac{\partial \beta}{\partial y} \frac{\partial v}{\partial x} \\
 & + \gamma_{11} \frac{1}{\beta^2} \frac{\partial \beta}{\partial z} \frac{\partial w}{\partial x} + \gamma_{12} \frac{1}{\beta} \frac{\partial g}{\partial x} \frac{\partial v}{\partial y} + \gamma_{13} \frac{1}{\beta} \frac{\partial g}{\partial x} \frac{\partial w}{\partial z} \left. \right] + \left(\frac{2\kappa(\gamma - 1)}{R\gamma} \right)^2 \frac{1}{\rho\beta} \left[\gamma_{14} \frac{\partial \beta}{\partial y} \frac{\partial v}{\partial x} + \gamma_{15} \frac{\partial \beta}{\partial z} \frac{\partial w}{\partial x} \right. \\
 & \left. + \gamma_{16} \frac{\partial \beta}{\partial x} \frac{\partial u}{\partial x} + \gamma_{17} \frac{\partial \beta}{\partial y} \frac{\partial u}{\partial y} + \gamma_{18} \frac{\partial \beta}{\partial z} \frac{\partial u}{\partial z} + \gamma_{19} \frac{\partial \beta}{\partial x} \frac{\partial v}{\partial y} + \gamma_{20} \frac{\partial \beta}{\partial x} \frac{\partial w}{\partial z} \right],
 \end{aligned}$$

$$\text{where, } \beta = \frac{1}{2RT}, \quad g = \log \left(\frac{\rho}{\beta} \right)$$

Singh et al., Derivation of stable Burnett equations for rarefied gas flows, PRE (2017)

Advantages of Proposed Approach

- Additional boundary conditions not required
 - OBurnett equations are 2nd order!
- Stress terms are not dependent on temperature gradient
- Derived equations are unconditionally stable
- Accounts for non-unity Prandtl number

Proposed equations appear to be physically more consistent

Validation of Proposed OBurnett Equations

- Couette flow
- Force driven Poiseuille flow
- Pressure driven Poiseuille flow

Forced driven Poiseuille flow using OBurnett equations

Assumptions

- The velocity normal to the stationary walls, v is zero.
- The third component of velocity, w is zero, owing to the flow being two-dimensional.
- All the flow variables are functions of y -direction only.

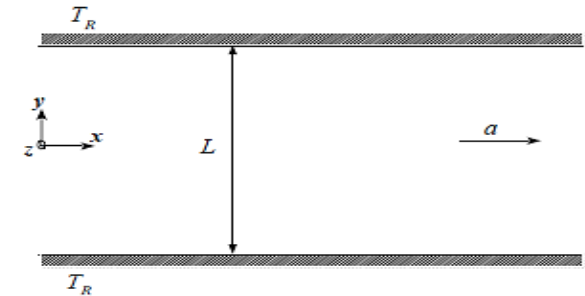
Governing Equations

$$\frac{d^2 u^*}{ds^2} = -\frac{1}{2T^*} \frac{dT^*}{ds} \frac{du^*}{ds} + \frac{b'_0 p^*}{T^{*3/2}},$$

$$\frac{dp^*}{ds} = \frac{\left\{ -\frac{2T^*}{p^*} \frac{du^*}{ds} \left[-\frac{1}{2T^*} \frac{dT^*}{ds} \frac{du^*}{ds} + \frac{b'_0 p^*}{T^{*3/2}} \right] + \left(\frac{du^*}{ds} \right)^2 \frac{1}{p^*} \frac{dT^*}{ds} \right\}}{\left\{ b'_2 - \frac{T^*}{p^{*2}} \left(\frac{du^*}{ds} \right)^2 \right\}},$$

$$\frac{d^2 T^*}{ds^2} = -\frac{8c_\mu}{15c_\lambda} \left(\frac{du^*}{ds} \right)^2 - \frac{1}{2T^*} \left(\frac{dT^*}{ds} \right)^2.$$

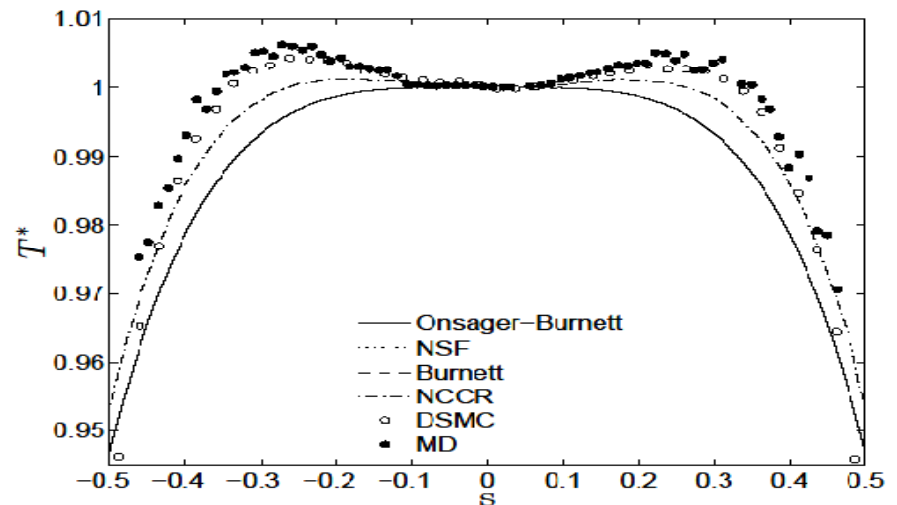
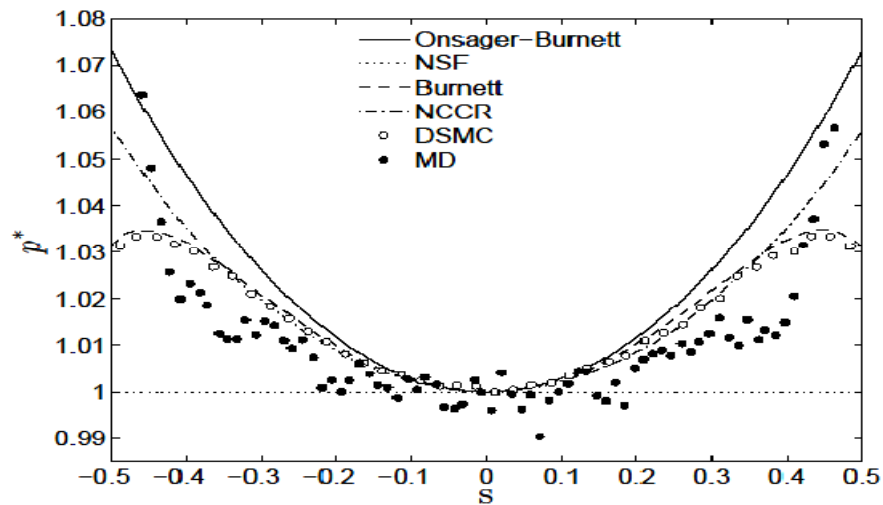
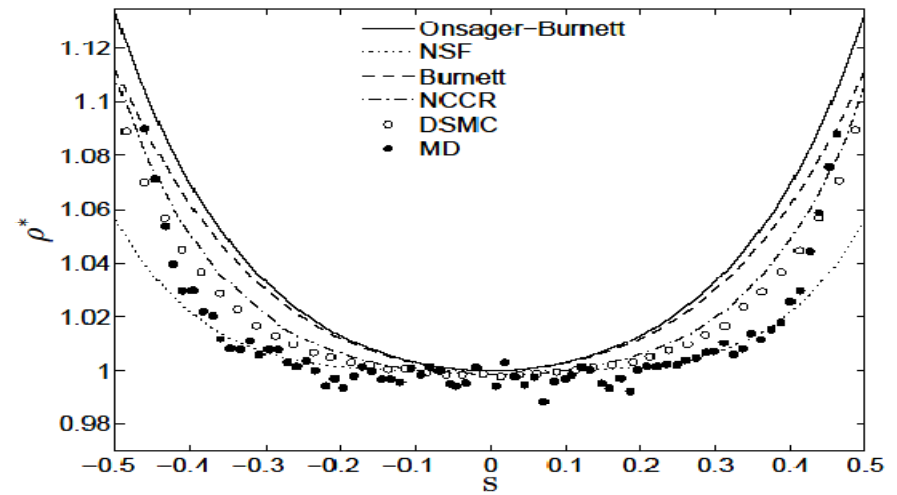
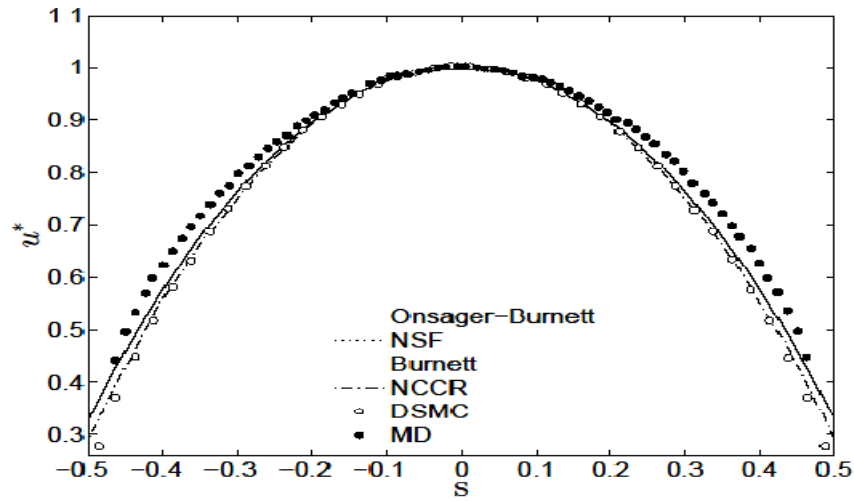
Jadhav et al., Force-driven compressible plane Poiseuille flow by Onsager-Burnett equations, PoF (2017) (**Editor's pick** article)



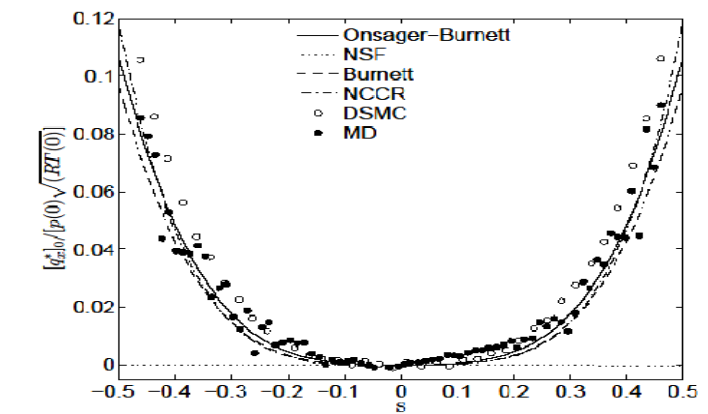
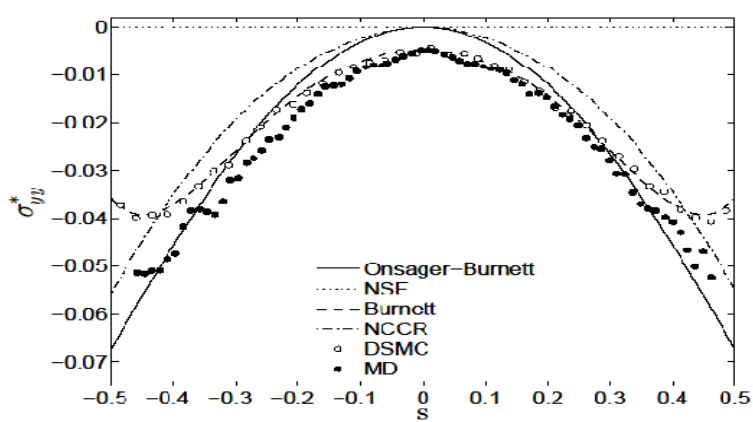
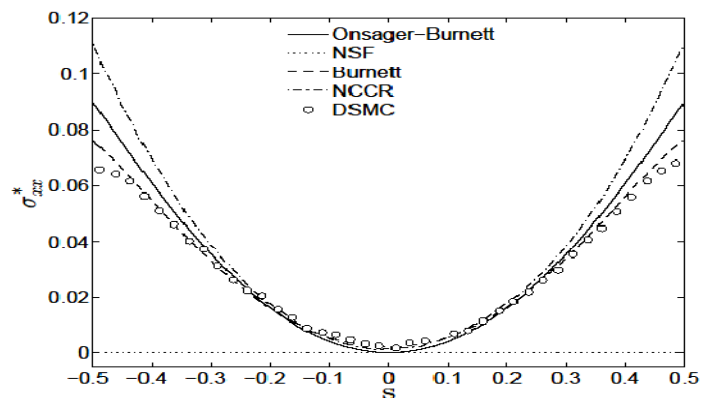
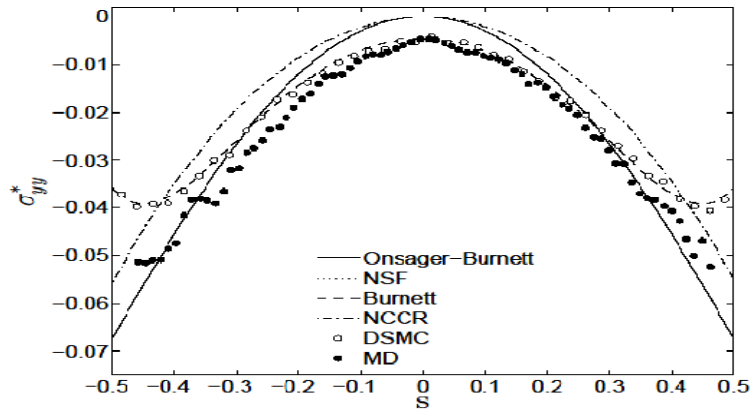
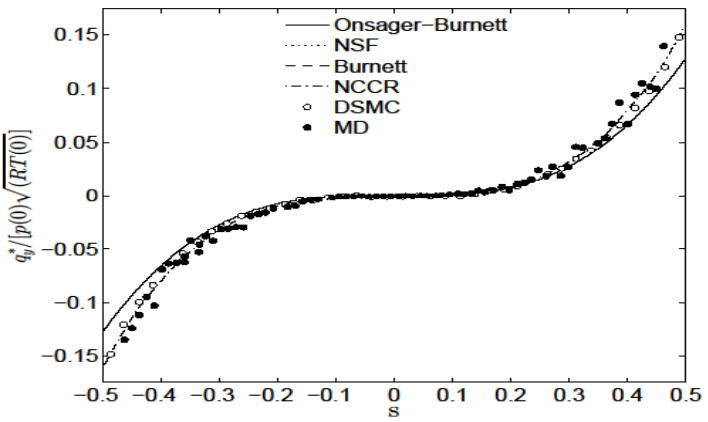
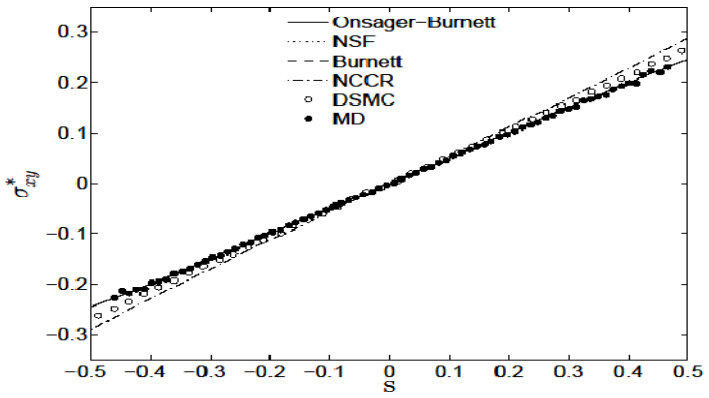
Schematic of plane Poiseuille flow driven by external force, 'a'

Ref: Uribe and Garcia, PRE 1999

Conserved variables: u^* , ρ^* , p^* and T^*



Non-conserved variables: σ_{xy}^* , q_y^* , σ_{yy}^* , σ_{xx}^* , σ_{zz}^* and q_x^*



Jadhav et al., Force-driven compressible plane Poiseuille flow by Onsager-Burnett equations, PoF (2017) (Editor's pick article)

Summary

Blood plasma separation microdevice

- eliminates the need for centrifugation
- demonstrated on whole blood

Three-dimensional hydrodynamic focusing microdevice

- simple design
- requires fewer number of accessories

Beyond Navier-Stokes equations

- Possible to solve Burnett equations analytically ($Kn \sim 2.2$)
- Proposed new set of Burnett-type higher-order continuum transport equations (super-set of Navier-Stokes equations)

Acknowledgements

Students

- Dr. Siddhartha Tripathi, Varun Kumar, Dr. Amit Prabhakar, Nishant Kumar – BPS Device
- Dr. Siddhartha Tripathi, Varun Kumar – HF Microdevice
- Narendra Singh, Ravi Jadhav – for theoretical work

Funding

- DAE-SRC Outstanding Investigator Award
- IRCC, IIT Bombay
- Department of Science and Technology, New Delhi
- WRCB, IIT Bombay

Thank You!